Gab2 Promotes Colony-Stimulating Factor 1-Regulated Macrophage Expansion via Alternate Effectors at Different Stages of Development[▽]

Angel W. Lee,[1,2]* Yingwei Mao,[1]† Josef M. Penninger,[3] and Soojie Yu[1]‡

Department of Pharmacology, The University of Michigan Medical School, Ann Arbor, Michigan[1]; The Institute of Molecular
Medicine, The University of Texas Health Sciences Center at Houston, Houston, Texas[2]; and Institute of
Molecular Biotechnology, The Austrian Academy of Sciences, Vienna, Austria[3]

Colony-stimulating factor 1 (CSF-1) receptor (CSF-1R, or macrophage CSF receptor [M-CSFR]) is the primary regulator of the proliferation, survival, and differentiation of mononuclear phagocytes (MNPs), but the critical CSF-1 signals for these functions are unclear. The scaffold protein Gab2 is a major tyrosyl phosphoprotein in the CSF-1R signaling network. Here we demonstrate that Gab2 deficiency results in profoundly defective expansion of CSF-1R-dependent MNP progenitors in the bone marrow, through decreased proliferation and survival. Reconstitution and phospho-flow studies show that downstream of CSF-1R, Gab2 uses phosphatidylinositol 3-kinase (PI3K)-Akt and extracellular signal-regulated kinase (Erk) to regulate MNP progenitor expansion. Unexpectedly, Gab2 ablation enhances Jun N-terminal protein kinase 1 (JNK1) phosphorylation in differentiated MNPs but reduces their proliferation; inhibition of JNK signaling or reduction of JNK1 levels restores proliferation. MNP recruitment to inflammatory sites and the corresponding bone marrow response is strongly impaired in Gab2-deficient mice. Our data provide genetic and biochemical evidence that CSF-1R, through Gab2, utilizes different effectors at different stages of MNP development to promote their expansion.

Mononuclear phagocytes (MNPs) are critical in health to maintain tissue homeostasis and in disease as major effectors of innate immunity (7, 44). In the adult animal, MNPs develop from progenitors in the bone marrow (BM) that differentiate to monocytes (MOs), tissue macrophages (Mϕs), and specialized cells, including dendritic cells and osteoclasts. The human body makes >10^9 MOs/day and more under stress (59). Understanding the mechanisms regulating MNP production is essential not only to myelopoiesis but also inflammation.

Colony-stimulating factor 1 (CSF-1) acts on the receptor tyrosine kinase CSF-1 receptor (CSF-1R) and is the primary cytokine regulating the proliferation, survival, and differentiation of MOs, Mϕs, and osteoclasts (44, 52). CSF-1 is also critical to dendritic and Langerhans cell expansion (15, 35). A recently discovered, less potent ligand for the CSF-1R, interleukin-34 (IL-34), has a spatiotemporal expression pattern different from CSF-1 during mouse development (63) and may be involved in microglial development (14). CSF-1-null (op/op) (64) and CSF-1R-null (9) mice have severe deficiencies in hematopoietic progenitors, MOs, and Mϕs (7, 9, 65) and exhibit pleiotropic defects in innate immunity (4, 43), bone remodeling (9, 64), fertility (8), and tissue homeostasis (7). Moreover, CSF-1-regulated Mϕ infiltration underlies the

pathogenesis of chronic inflammatory diseases (7). In a polyoma middle-T mouse model for breast cancer, ablation of CSF-1 reduces tumorigenesis and metastatic potential (46). CSF-1 serum levels are tens of nanograms per milliliter (18), making CSF-1 an important contributor to immune responses through trophic support and activation of MNPs.

Deciphering how the body controls MNP production and function will require detailed mechanistic knowledge of CSF-1, CSF-1R, and their downstream effectors. Using the 32D myeloid progenitor cell line transfected with the CSF-1R (32D.R), we previously showed that full activation of phosphatidylinositol 3-kinase (PI3K)-Akt and mitogenesis requires a feed forward amplification loop involving Gab2 (28, 31). Gab2 is a member of the Gab family of scaffolding proteins (Gab1 to -3) that modulate and amplify signals from numerous cell surface receptors (19, 34, 38). They have a pleckstrin homology domain for membrane localization, tyrosines for recruiting PI3K and SHP2, and proline-rich domains for binding Grb2. Gab2$^{-/-}$ mice have reduced numbers of mast cells (68) and exhibit abnormal allergic responses (21) and defective competitive BM repopulation (70). Similar to CSF-1-null and CSF-1R-null mice, Gab2$^{-/-}$ mice are osteopetrotic (24, 61) because of impaired RANKL signaling (61). An important role for Gab2 has been demonstrated in juvenile myeloproliferative leukemia (66), breast cancer (10, 27), and Alzheimer's disease (47). The latter two diseases have prominent inflammatory features, and it is not known if Gab2 is mediating its effects through MNPs.

Herein, we demonstrate that Gab2 is the major Gab family member promoting CSF-1-dependent proliferation in MNPs. Using BM cells from Gab2$^{-/-}$ mice, we show that Gab2 is required for maximal CSF-1-dependent MNP precursor ex-

* Corresponding author. Present address: OncProTech, P.O. Box 2501, Ann Arbor, MI 48106-2501. Phone and fax: (734) 786-3876. E-mail: awmlee@angelleelab.org.
† Present address: Biology Department, Penn State University, State College, PA 16802.
‡ Present address: The Ohio State University College of Medicine, Columbus, OH 43210.

pansion, by supporting survival and proliferation of purified CD31^{high} Ly6C^{−} myeloid progenitors. Mechanistically, we demonstrate a key role for the combined actions of Gab2-regulated PI3K-Akt and SHP2-extracellular signal-regulated kinase (Erk) axes in the expansion of MNP progenitors. Gab2 deficiency also reduces the mitogenic response to CSF-1 during terminal MO/Mφ differentiation. In contrast to MNP progenitors, Gab2's function in differentiated Mφs is independent of Akt and Erk as well as Stat3/5 but dependent on Jun N-terminal protein kinase 1 (JNK1) signaling. Thus, Gab2 controls the entire process of CSF-1 dependent MNP formation in the BM; however, Gab2 may mediate its effects on proliferation/differentiation using different effectors at different stages. Lastly, Gab2 was shown to contribute to Mφ recruitment in acute inflammation, in part through regulating the BM response.

MATERIALS AND METHODS

Reagents. Recombinant human CSF-1 (rhCSF-1) was a gift from Genetics Institute. Murine IL-3 and stem cell factor (SCF) were from Peprotech, Inc. We used the following antibodies: Gab2, phosphotyrosine (4G10), and CSF-1R from Upstate Biotechnology; Gab1, Gab3, SHP2, Erk, JNK1, and AKT1 from Santa Cruz Biotechnology; and phospho-specific antibodies and antibodies to JNK2 and mitogen-activated protein kinase (MAPK) kinase 7 (MKK7) from Cell Signaling. For immunoblotting, we used pAktT308 (9275), pAktS473 (9271), pErk (9106), pStat3 (9138), and pStat5 (9356). For flow cytometry, we used pAktS473 (4058), pErk (4377), and pS6 (2211). We obtained a Gab2 antiserum raised against full-length Gab2 from T. Hirano (Osaka University) and a Gab3 antiserum from L. Rohrschneider (Fred Hutchinson Cancer Research Center). F4/80 antibodies were from Serotec. Anti-JNK1/2 and all other antibodies for fluorescence-activated cell sorting (FACS) were from BD Biosciences or eBioscience. We used the following clones for FACS: F4/80 (C1:A3-1), Ly6C (AL-21), Ly6G (1A8), CD31 (MEC13.3), CSF-1R/CD115 (AFS98), c-Kit/CD117 (2B8), Flt3/CD135 (A2F10), CD16/32 (93), CD34 (RAM34), Sca-1 (D7), CD11b (M1/70), Gr-1 (RB6-8C5), CD4 (GK1.5), CD8α (53-6.7), CD19 (1D3), CD127 (A7R34), and Ter119. The JNK peptide inhibitor (JNKI-1) was from Calbiochem. 7-Aminoactinomycin D (7-AAD) and 4′,6-diamidino-2-phenylindole, dilactate (DAPI), were from Molecular Probes.

Animals. Gab2^{−/−} mice have been described previously (61) and were further backcrossed to a C57BL/6 background at the University of Michigan for an additional 5 generations for a total of 9 backcrosses. Animals were used between 7 and 10 weeks of age. Mice were housed in a specific-pathogen-free environment. The Animal Welfare Committees at the University of Michigan and the University of Texas Health Science Center, Houston, approved all animal protocols.

Cell culture. The 32D.R cell line expressing CSF-1R has been described previously (29). Total BM cells were induced to differentiate to Mφs as described previously (28). BM cells were harvested by flushing both femurs, tibias, and iliac crests and counted using a hemocytometer after red blood cell (RBC) lysis. They were plated in a mixture of minimal essential medium alpha (αMEM), 15% fetal bovine serum (FBS), and 50 μM β-mercaptoethanol (BM medium), containing 12 ng/ml CSF-1 and 15 ng/ml IL-3. After overnight culture, nonadherent cells were layered over a Ficoll-Hypaque gradient, and the mononuclear fraction was plated in BM medium with 12 ng/ml CSF-1 and 5 ng/ml IL-3. After another 24 h, nonadherent cells were harvested and seeded in 30% L cell conditioned medium and 20 ng/ml CSF-1. To obtain the LIN*[−] population, D2 BM cells were stained with antibodies to CD4, CD8, CD19, Ter119, and Ly6G and depleted by magnetically activated cell sorting (MACS; Miltenyi). We used the 1A8 Ly6G antibody to exclude granulocytes since the Gr1 antibody recognizes both Ly6G and Ly6C (13). We excluded the CD11b antibody from the depletion cocktail since CD11b is expressed on more mature MNP precursors (32). In some experiments, LIN*^{−} cells were sorted for the CD31^{high} Ly6C^{−} subset. To obtain early CSF-1-responsive progenitors directly from the mouse, we followed a previously described procedure (57) which specifically excludes Ly6C^{+} cells since Ly6C is expressed on more mature MNP precursors. Briefly, total BM cells were lineage depleted by MACS with antibodies to CD11b, CD4, CD8α, CD19, Ter119, CD127, Gr1, and F4/80. Lineage-depleted (LIN^{−}) cells were stained with c-Kit–allophycocyanin (APC), CD31-phycoerythrin (PE), Ly6C-fluorescein isothiocya-

nate (FITC), and goat anti-rat–FITC antibodies and sorted for c-Kit^{+} CD31^{high} cells in the FITC^{−} fraction on a Vantage SE or FACSAria (BD Biosciences). Sorted cells (LIN^{−} c-Kit^{+} CD31^{high} Ly6C^{−}, abbreviated LK31C) were >90% pure and plated in BM medium with 100 ng/ml CSF-1. In experiments where LK31C cells were further distinguished based on Flt3 expression, LIN^{−} cells were stained with c-Kit-PECY7, CD31-APC, Ly6C-FITC, and Flt3-PE antibodies for sorting. Nonviable cells were excluded by 7-AAD staining.

Plasmids, transfections, and viral transductions. WT, 3YF, and DM Gab2 cDNAs (20) were cloned into pMSCV-IRES-EGFP (42). Short hairpin RNAs (shRNAs) targeting the 3′ untranscribed region (UTR) of murine Gab2 and Gab3 cloned into pU6 or pLentiLoX have been described (36). dsRed was substituted for green fluorescent protein (GFP) in pLentiLoX to create pLentiLoX-dsRed. MISSION lentiviral shRNAs targeting murine JNK1 were cloned into pLKO.1 (shJNK1-1, TRCN0000012583; shJNK1-2, TRCN0000012585; shJNK1-3, TRCN0000012584; shJNK1-4, TRCN0000012586 [Sigma-Aldrich]). Ecotropic retroviruses and vesicular stomatitis virus G (VSVG)-pseudotyped lentiviruses were produced in 293T cells (36). 32D.R cells were electroporated with pU6-shGab2 and pPUR (Clonetech) or transduced with GFP-shGab2 or dsRed-shGab3 lentiviruses separately or together and flow sorted based on GFP or dsRed expression. Individual clones were isolated. Clones that were transfected/transduced with shXASH (XASH is an irrelevant frog protein) (36) or with shGab2 but showed no knockdown (sham) were used as controls. To transduce BM cells with pMSCV retroviruses, total BM cells were cultured in IL-3 and CSF-1 for 24 h prior to 3 rounds of 1 h of spin infection over 24 h, and 48 h after initial isolation, the cells were sorted for GFP expression. Day 5 (D5) bone marrow-derived macrophages (BMMs) were spin infected with pMSCV retroviruses and sorted 48 h later for GFP expression. For transduction with JNK1 shRNAs, after spin infection on D3, BM cells were cultured in CSF-1 for 2 days prior to the addition of 4 μg/ml puromycin (Sigma). Cells were selected in puromycin for 48 h and washed extensively, and viable cells were used for experiments.

FACS analysis. BM cells were labeled with 2 μM carboxyfluorescein diacetate succinimidyl ester (CFSE cell tracer kit; Molecular Probes). CFSE-labeled cells were stained with ethidium monoazide to exclude nonviable cells prior to fixation with 2% paraformaldehyde (41). To analyze apoptosis and cell cycle progression, sorted LIN*^{−} CD31^{high} Ly6C^{−} cells were immediately plated in BM medium containing CSF-1. Both floating and adherent cells were collected 72 h after plating and stained with CD11b-APC, annexin V-FITC, and propidium iodide. For cell cycle analysis, 48 h after plating, cells were washed and starved for 24 h in BM medium containing reduced amounts of CSF-1 (4 ng/ml) to avoid cell death but prevent cell proliferation. CSF-1 (400 ng/ml) was then added for an additional 27 h. Bromodeoxyuridine (BrdU; 10 μM) was added during the last 6 h of incubation. Cells were blocked and stained with CD11b-APC before processing for bromodeoxyuridine uptake (BrdU flow kit; BD Biosciences). BMMs were fixed in 80% ethanol and stained with 2 μg/ml Hoechst 33258 (Sigma) and 4 μg/ml of pyronin Y (Polysciences). For immunophenotyping, 7-AAD or DAPI was used as a viability marker for unfixed cells. Otherwise, cells were stained with Live/Dead fixable violet or near-infrared (near-IR) fluorescent dye (Invitrogen) prior to fixation in BD stabilizing fixative. Cells were blocked with CD16/32 (FcγRII/III) antibodies for 10 min on ice prior to staining. Data were acquired on a BD FACSCalibur, LSR II, or FACSAria II. Gating was based on isotype or fluorescence minus one (FMO) (41) controls.

FACS analysis of intracellular signaling. Freshly purified LIN*^{−} cells were deprived of serum and growth factors for 3 h prior to CSF-1 stimulation. Inhibitors were added during the last hour of starvation. Cells were fixed in 1.5% paraformaldehyde for 10 min, resuspended in phosphate-buffered saline (PBS) plus 2% bovine serum albumin (BSA), and incubated on ice for 45 min. Cells were blocked for 15 min and then incubated for 30 min ± anti-Ly6C–FITC, followed by permeabilization in ice-cold methanol before storage at −80°C overnight. Staining with anti-Ly6C–FITC must occur prior to permeabilization to preserve the CD31 and Ly6C subsets, whereas anti-CD31–PE must be used after methanol, which would otherwise destroy its fluorescence. Samples were processed for staining with CD31-PE and rabbit phospho- and donkey anti-rabbit–APC antibodies and analyzed immediately on a BD FACSCanto. A minimum of 10,000 events in each subset was collected at every time point. FMO controls were used to set the gates, and signaling inhibitors were used to confirm the authenticity of the phospho signal. Between 3×10^5 and 5×10^5 LIN*^{−} cells were used for each FACS sample.

All FACS data were analyzed with FlowJo (Treestar).

Clonogenic and proliferation assays. For assessment of the number of CSF-1-dependent CFU (CFU-C) (1a) total BM, D2 BM, or FACS-sorted cells were plated in duplicate in Methocult (M3231; Stem Cell Technologies) in the presence of 100 ng/ml CSF-1. In some experiments, SCF was added as a costimula-
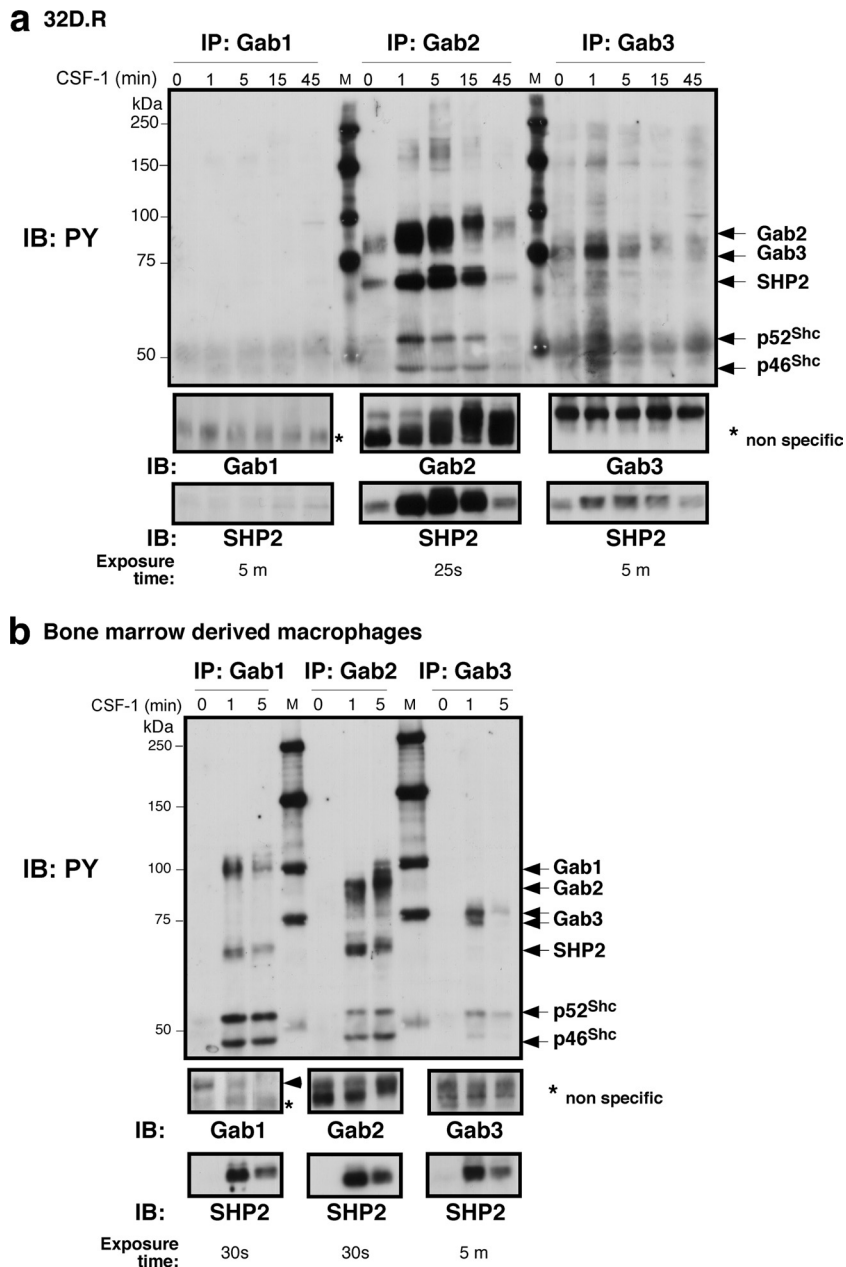
FIG. 1. CSF-1 signals to Gab proteins in 32D.R cells (a) and BM-derived macrophages (b), as shown by immunoprecipitation (IP) and immunoblotting (IB) analyses. Previously identified tyrosyl phosphoproteins are indicated. An arrowhead points to the authentic Gab1 band that comigrated with tyrosine-phosphorylated Gab1. PY, phosphotyrosine; M, molecular mass markers (kDa).

tory cytokine. Colonies greater than 50 cells were scored on D7. To assess myeloid colony potential, cells were plated in duplicate in Methocult containing premixed SCF, IL-3, IL-6, and erythropoietin (M3434; Stem Cell Technologies). Colonies were scored on D8. Photomicrographs were digitally acquired (DP70; Olympus), and the longest diameter of each colony was determined using a stage micrometer (ImageJ 1.43; NIH). To assess proliferation, the MTS [3-(4,5-dimethylthiazol-2-yl)-5-(3-carboxymethoxyphenyl)-2-(4-sulfophenyl)-2H-tetrazolium] assay (CellTiter 96 aqueous nonradioactive proliferation assay; Promega) was performed as described previously (28, 55). The 50% effective concentration (EC_{50}) was calculated using Prism 4. For BMMs, 3,750 D5 cells were seeded per well in triplicate in a 96-well tissue culture plate. 32D cells and BMMs were assayed after 48 h. In some experiments, JNKI-1 or U0126 (Cell Signaling) was added. Cell number increases were determined by counting duplicate wells using a hemocytometer and excluding dead cells by Trypan blue staining. For BMMs,

low-adhesion 24-well plates (Greiner CELLSTAR plates for suspension cells) were seeded with 2×10^4 D5 cells in BM medium with the amounts of CSF-1 indicated. At specified times, cells were removed completely by incubation on ice in PBS plus 2 mM EDTA and counted.

Protein analysis. D7 BMMs were deprived of CSF-1 for 12 h prior to stimulation with CSF-1. Lysis, immunoprecipitation, and immunoblotting were performed as previously described (31). Cell lysates were precleared with protein A-Sepharose beads that had been blocked with IgG. Gab2 immunoprecipitation was performed with an antiserum from T. Hirano and immunoblotted with a different Gab2 antibody from UBI. Gab3 levels in cell lysates were assessed by immunoprecipitation or immunoblotting since available Gab3 antibodies could not reliably detect Gab3 in lysates, as noted previously (51). In experiments with actinomycin D (AD), cells were pretreated for 10 or 15 min (see Fig. 11 legend) before CSF-1 addition.
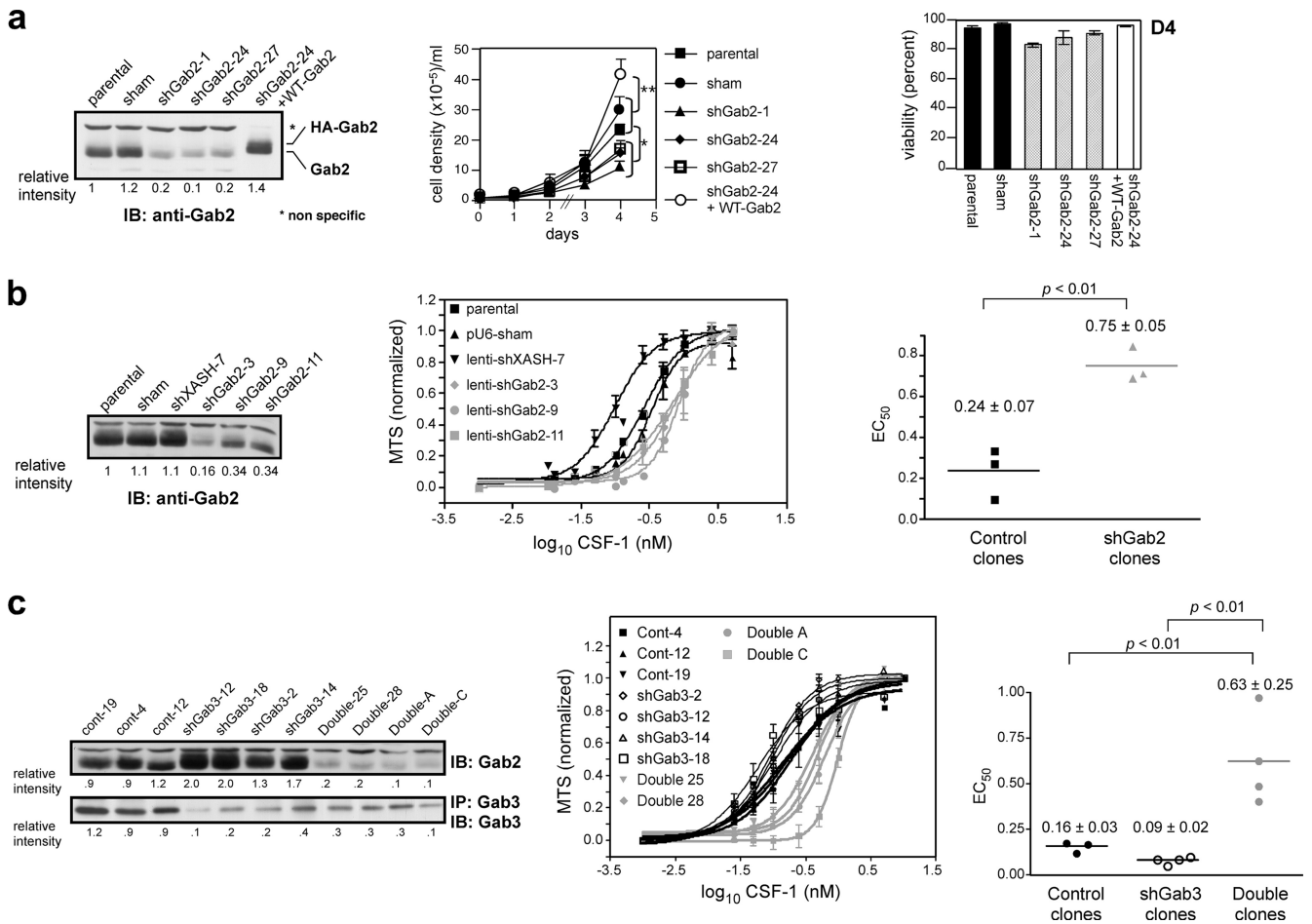
FIG. 2. Silencing of Gab2 but not Gab3 reduces CSF-1-dependent proliferation in 32D.R. (a) Gab2 knockdown with pU6 shRNA vectors. WT Gab2 was overexpressed in clone 24. Fifty micrograms was loaded except for WT Gab2 (5 μg). Growth curves and D4 viabilities were determined. The results are shown for 3 independent experiments. P values were calculated using the one-way analysis of variance (ANOVA) test. (b) Gab2 knockdown with shGab2 lentiviruses. Each CSF-1 MTS response curve is the average of 2 independent experiments. (c) Gab3 knockdown (shGab3) or combined Gab2 and Gab3 knockdown (Double) in 32D.R. Levels were normalized to the averaged control clones. Each CSF-1 response curve is averaged from 3 independent experiments. (b and c) MTS curves normalized to 0 to 1 for determination of EC_{50}. Control, thick black lines; shGab3, thin black lines; combined knockdown ("Double"), gray lines.

TG and LPS injection. Mice were injected intraperitoneally with 1 ml of 3% Brewer's thioglycolate (TG) (BD Diagnostic). Peritoneal lavage was performed with 2 × 5 ml of PBS plus 2% fetal bovine serum (FBS). For lipopolysaccharide (LPS), mice were injected intraperitoneally with 15 mg/kg LPS (0111:B4 from Sigma), and bone marrow was harvested 60 h later.

Statistical analysis. Prism 4 (GraphPad Software, Inc.) was used in statistical analyses. Except where stated, P values were calculated using the Student's 2-sided t test and indicated on the figures as follows: *, $P < 0.05$; **, $P < 0.005$; and ns, not significant. Averages are given as the mean ± standard deviation (SD).

RESULTS

Gab2 not Gab3 promotes CSF-1-dependent proliferation and Akt or Erk activation. CSF-1 stimulation of 32D.R myeloid progenitors induced Gab2-3 tyrosine phosphorylation and association with known partners, SHP2 and Shc (19, 31). Gab1 expression was undetectable (Fig. 1a). In BM-derived MΦs (BMMs), CSF-1 provoked the tyrosine phosphorylation of Gab1-3 (Fig. 1b). To determine if Gab proteins play overlapping roles in the myeloid lineage, we stably knocked down

Gab2 in 32D.R cells. Initially we cotransfected 32D.R cells with pU6 shRNAs and a puromycin selectable marker (36). Gab2 knockdown clones grew more slowly, but cell survival was not noticeably affected. Reconstitution with WT Gab2 cDNA lacking the shRNA target sequence restored proliferation (Fig. 2a). Since puromycin-resistant clones required 2 to 3 weeks of selection and expansion, we also used shRNA lentiviruses for rapid GFP-based isolation. MTS results showed that the EC_{50} for knockdown clones was 3.1-fold higher than that of the control (Fig. 2b). Reducing Gab3 expression was associated with increased Gab2 levels so that the resulting EC_{50} was slightly diminished relative to the control (Fig. 2c). When Gab2 and Gab3 were simultaneously silenced, the EC_{50} was 3.9-fold higher relative to the control. Hence, downregulation of Gab3 in addition to Gab2 had only a small effect. Thus, the CSF-1R uses primarily Gab2 to promote proliferation in 32D.R cells.

We and other groups have shown that Gab2 signals through the PI3K and/or Erk pathways (20, 31, 33, 36). However, mul-
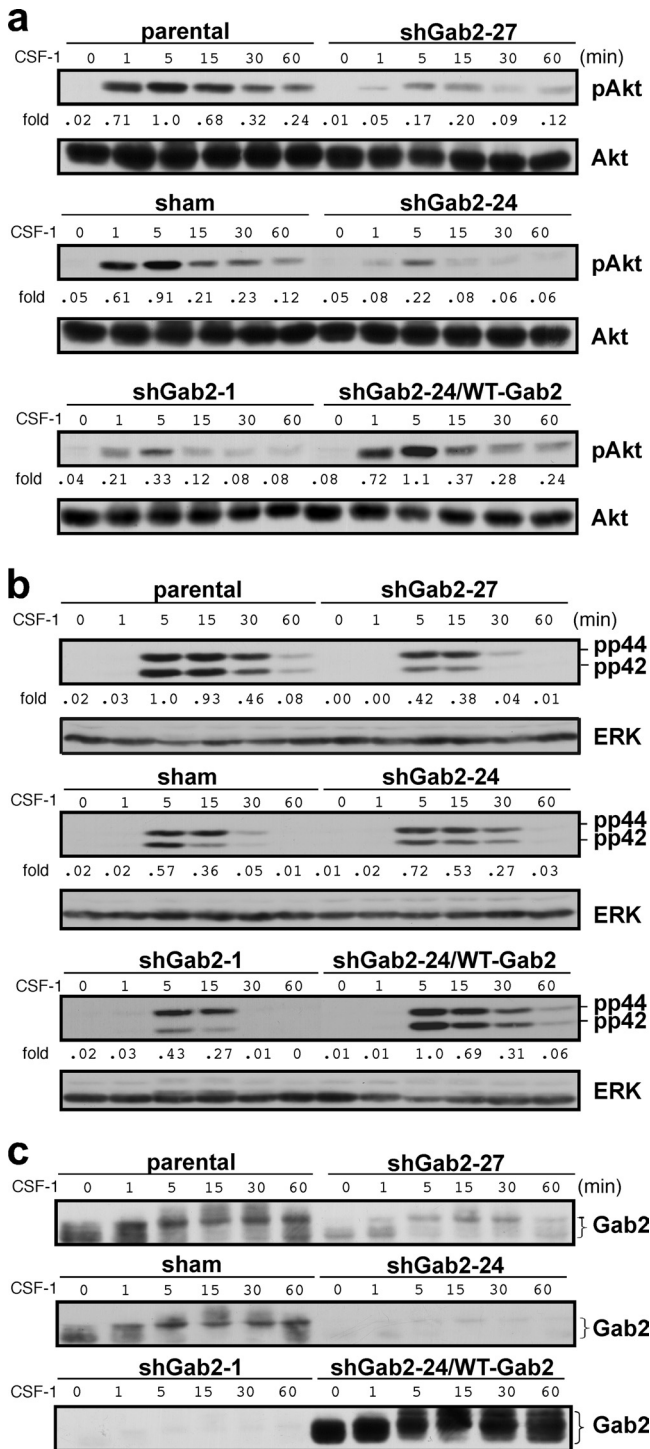
FIG. 3. Gab2 knockdown impacts CSF-1-mediated signaling in 32D.R cells. Separate immunoblots were performed for pAkt and total Akt (a), pErk and total Erk (b), and Gab2 (c). Shown are representative results for 1 of 2 independent experiments. Fold changes are relative to the phosphorylation of parental cells 5 min after CSF-1 addition.

tiple pathways can lead to CSF-1R-mediated activation of PI3K and Erk (23, 28, 31, 43). Gab2 silencing in 32D.R reduced CSF-1-provoked Akt phosphorylation that was restored by reexpression of WT Gab2 (Fig. 3a). Although we did not see

a consistent reduction in Erk phosphorylation in the knock-down clones (Fig. 3b), reintroduction of WT Gab2 enhanced Erk phosphorylation, supporting a role for Gab2 in Erk regulation. Control and Gab2 knockdown clones obtained by lentiviral transduction showed results similar to the pU6 clones. Thus, in 32D.R cells, CSF-1 depends in part on Gab2 to activate Akt and, to a lesser degree, Erk and to promote proliferation.

Gab2-deficient BM has reduced numbers of MOs, Mϕs, and CSF-1-responsive CFU. When BM cells were induced by CSF-1 to differentiate to Mϕs, Gab2 expression increased markedly (Fig. 4a). To determine if Gab2 deficiency could adversely impact the MNP lineage *in vivo*, we used an F4/80 antibody (16, 32) to identify MOs and Mϕs in WT and Gab2$^{-/-}$ BM. Gab2$^{-/-}$ BM showed a modest decrease in the percentage of F4/80$^+$ cells compared to that in WT mice (Fig. 4b). Consistent with previous findings (61), Gab2$^{-/-}$ mice had fewer BM cells (Table 1); consequently, the overall reduction in F4/80$^+$ cells in Gab2$^{-/-}$ mice was more marked. Additionally, not all F4/80$^+$ MOs or Mϕs are lost from the BM of CSF-1R-null mice (9); therefore, we are probably underestimating the impact of Gab2 deletion on CSF-1 mediated MNP development. Staining for CSF-1R, which is expressed in MNPs and their precursors, revealed a similar reduction in the absence of Gab2 (Fig. 4c; Table 1).

Our results from 32D.R progenitors suggest that Gab2 deficiency could affect CSF-1-supported BM progenitor proliferation. The CFU-C assay detects the earliest BM progenitor that can respond to CSF-1 alone (37, 52). In WT mice, 1 in 10^3 nucleated BM cells gave rise to a CFU-C (Fig. 4d). Gab2$^{-/-}$ mice had a >7-fold reduction in CFU-C numbers, and the colonies were much smaller. CSF-1 must synergize with other growth factors to commit multipotent progenitors to the MNP lineage (43, 54). After 48 h in CSF-1 and IL-3, the CFU-C frequency increased to 1 in 83, with cells from Gab2$^{-/-}$ mice showing an 8.5-fold reduction in CFU-C numbers (Fig. 4e). Cells in the CFU-C showed typical Mϕ morphology, and all cells expressed CSF-1R (not shown). BMMs from WT and Gab2$^{-/-}$ mice were also indistinguishable based on expression of CSF-1R, CD11b, F4/80, and PU.1, a transcription factor required for Mϕ development (25) (data not shown). Thus, under steady-state conditions, Gab2 is required for the optimal production of CSF-1-responsive BM progenitors and their proliferation but not for terminal differentiation.

Gab2-deficient BM has reduced numbers of CD31$^+$ progenitors and shows accelerated appearance of Ly6C$^+$ MOs. Leenen used the CD31 and Ly6C markers to define distinct stages of MNP development (11, 32). To characterize the CD31 and Ly6C subsets in our system, they were isolated from D2 BM cells by flow sorting (Fig. 5a). Most of the CFU-C were found in the CD31^{high} Ly6C$^-$ subset, with many fewer found in the CD31$^+$ Ly6C$^+$ subset, consistent with the presence of more mature cells of the MNP lineage in the latter (not shown). For days 1 to 3 after differentiation induction, Gab2$^{-/-}$ BM cells gave rise to 2-fold fewer CD31$^+$ Ly6C$^+$ precursors compared to the WT control (Fig. 5b and c). A difference was also noted in the more immature CD31^{high} Ly6C$^-$ subset (D2, 7.8 ± 1.2 versus 5.4 ± 1.4; $P < 0.05$). A CD31$^-$ Ly6C^{high} subset found on D0 had mostly disappeared by D1, consistent with these cells being MOs that had adhered
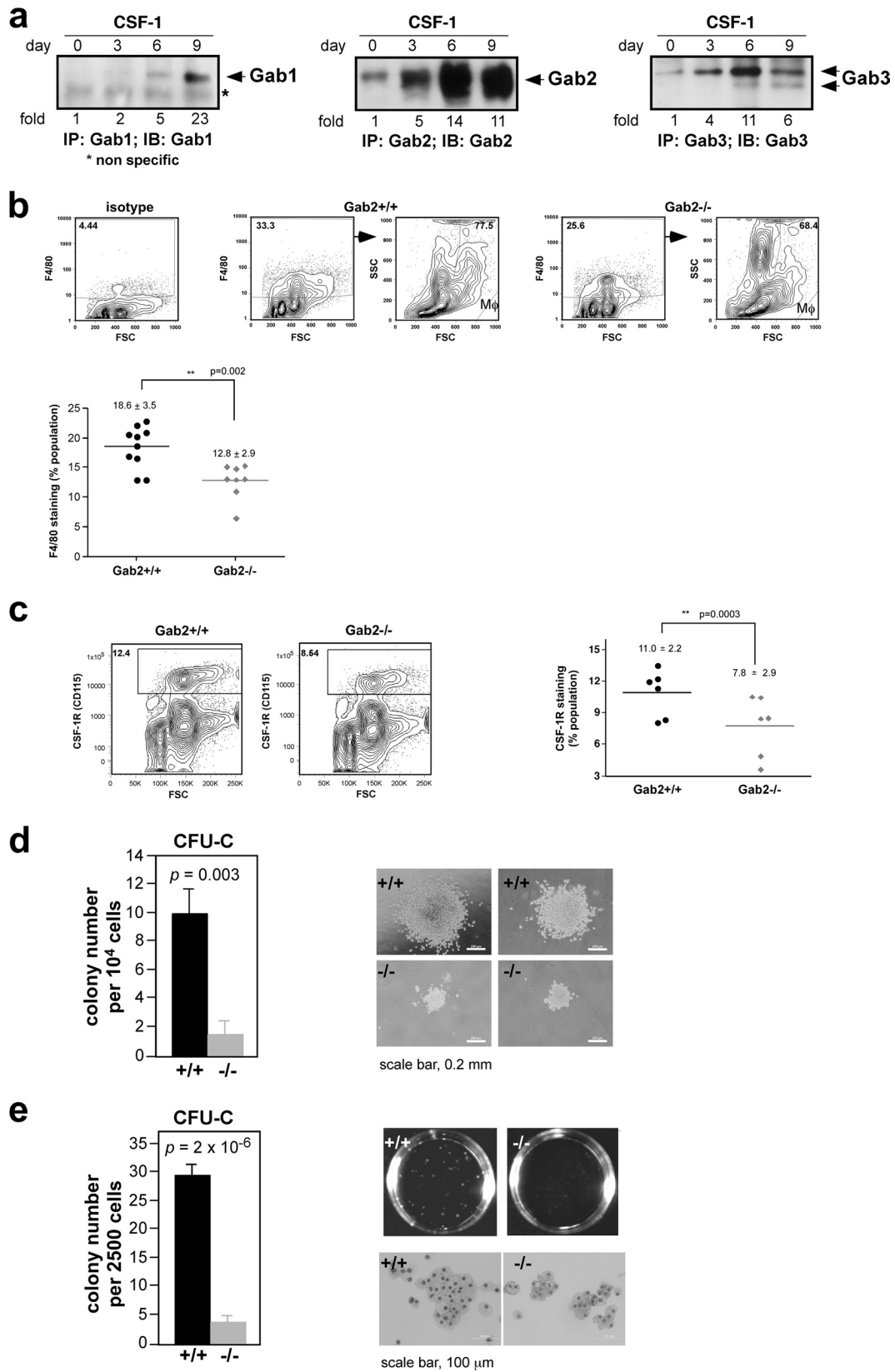
FIG. 4. BM from Gab2^{−/−} mice has fewer macrophages and shows impaired CSF-1-dependent colony-forming activity. (a) Total BM cells were induced to differentiate along the MNP lineage. (b) Nucleated BM cells were stained with F4/80 antibody and analyzed by flow cytometry. The percentage of F4/80^{+} BM cells from individual mice is shown, with background staining from an isotype control subtracted from each measure-

TABLE 1. F4/80$^+$ and CSF-1R$^+$ bone marrow cells in Gab2$^{+/+}$ and Gab2$^{-/-}$ mice

Mice	% of cells[b]:		Total no. of bone marrow cells (n)[a]	Mean age of mice (days)	Total no. of cells:	
	SSC$^{low-int}$ F4/80$^+$	CSF-1R$^+$			SSC$^{low-int}$ F4/80$^+$	CSF-1R$^+$
Gab2$^{+/+}$	18.6 ± 3.5	11.0 ± 2.2	(9.46 ± 0.47) × 10^7 (39)	66.9 ± 3.8	(1.76 ± 0.21) × 10^7	(1.04 ± 0.17) × 10^7
Gab2$^{-/-}$	12.8 ± 2.9	7.8 ± 2.9	(7.49 ± 0.31) × 10^7 (37)	68.5 ± 4.8	(9.58 ± 1.5) × 10^6	(5.84 ± 2.0) × 10^6

[a] The difference in the number of total nucleated bone marrow cells between Gab2$^{+/+}$ and Gab2$^{-/-}$ mice is significant ($P = 0.009$, unpaired t test). Shown are means and 95% confidence intervals.

[b] See Fig. 4. SSC$^{low-int}$, low to intermediate side scatter.

and removed from culture. By D2, MOs had reappeared in Gab2$^{-/-}$ but not WT cells. CD31$^-$ Ly6C$^+$ cells present on D0 were mainly granulocytes that were not completely eliminated on D2. By D5, cells were mostly CD31$^-$ Ly6C^{high} MOs and CD31$^-$ Ly6C$^-$ Mφs (11). The CD31$^-$ Ly6C$^+$ cells on D5 were MNPs, not granulocytes that had died off. By D7, most Gab2$^{-/-}$ cells were Ly6C$^-$ Mφs, whereas a significant number of WT cells were still Ly6C$^+$. Similar results were obtained using CD31 and CD11b, a pan myeloid marker that is expressed on Mφs (Fig. 5d). The diminished numbers of immature CD31^{high} Ly6C$^-$ and more mature CD31$^+$ Ly6C$^+$ progenitors along with the premature appearance of CD31$^-$ Ly6C^{high} MOs on D2 and the almost complete disappearance of MOs on D7 in the absence of Gab2 demonstrate that Gab2 is important for MNP expansion and timely differentiation.

We used lineage depletion to enrich for the CD31^{high} Ly6C$^-$ subset that contains the earliest, CSF-1-responsive progenitors (11) (Fig. 5e). Consistent with CSF-1R expression increasing with commitment and differentiation (48), the more immature LIN*$^-$ CD31^{high} Ly6C$^-$ subset showed a range of CSF-1R levels, whereas the more mature LIN*$^-$ CD31$^+$ Ly6C$^+$ subset has two distinct populations, with R2 expressing high levels of CSF-1R (Fig. 5f). R1 cells were CSF-1R$^-$ and had high side scatter (SSC), suggesting they were eosinophils not eliminated by depletion. Two-fold more LIN*$^-$ CSF-1R$^+$ CD31^{high} Ly6C$^-$ and LIN*$^-$ CSF-1R$^+$ CD31$^+$ Ly6C$^+$ precursors were present in WT compared to Gab2$^{-/-}$ cultures. Lineage depletion enriched the CFU-C in the LIN*$^-$ CD31^{high} Ly6C$^-$ subset to 1 in 35, and this subset from the Gab2$^{-/-}$ mice gave rise to ≈4-fold fewer CFU-C (Fig. 5g).
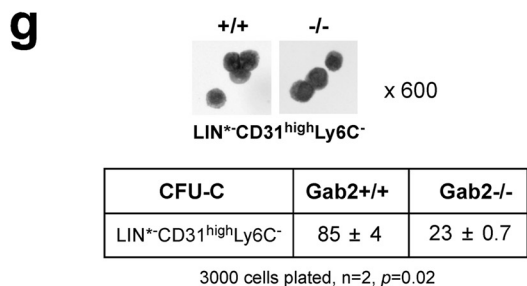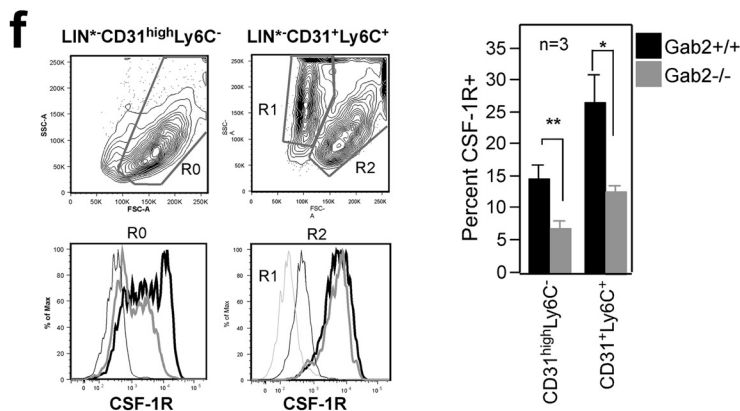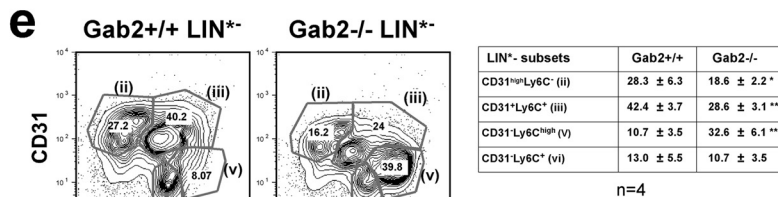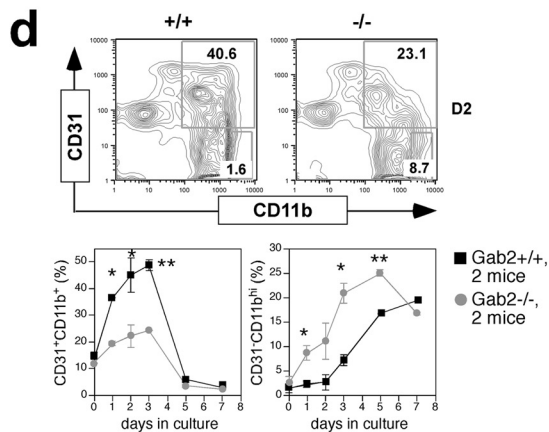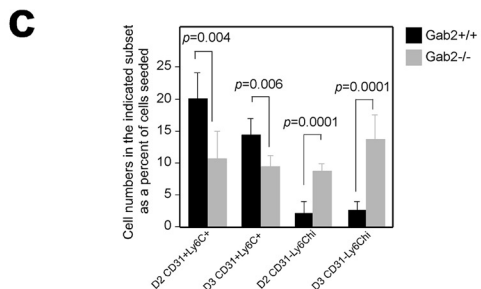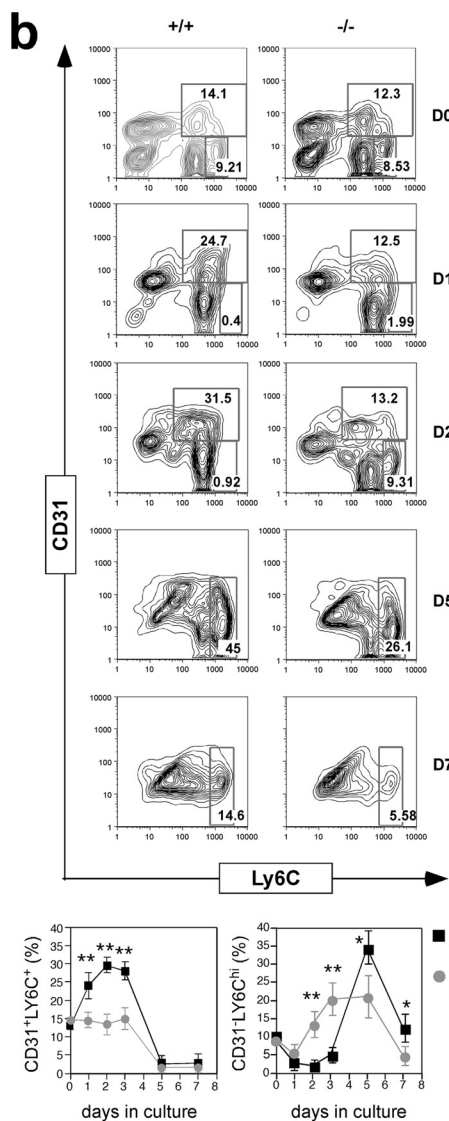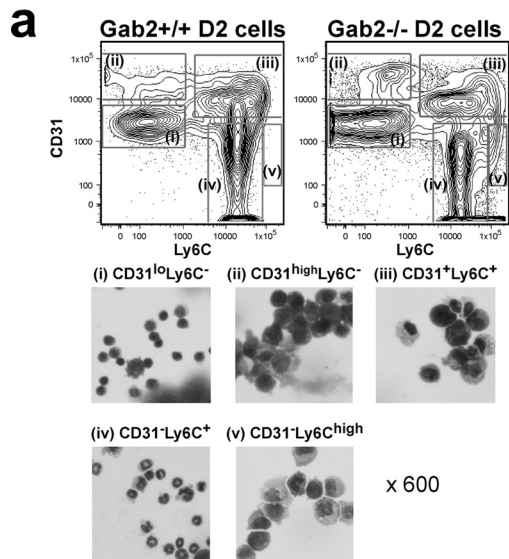
To verify that our findings in *ex vivo* expanded CSF-1-responsive BM progenitors also apply to MNP progenitors isolated directly from the BM, we purified early myeloid progenitors that can proliferate and differentiate in response to CSF-1 as LIN$^-$ c-Kit$^+$ CD31^{high} Ly6C$^-$ cells (LK31C) (Fig. 6a) (57). The frequency of CFU-C in LK31C was further enriched to 1 in 18, and a similar reduction was observed in CFU-C numbers in the LK31C subset from Gab2$^{-/-}$ mice, particularly at lower doses of CSF-1 (Fig. 6b). Addition of costimulatory cytokine SCF enhanced colony formation but did not correct the CSF-1 defect caused by Gab2 ablation. Cells in these colonies had Mφ morphology and were CSF-1R$^+$. We determined if the differ-

ence in CFU-C numbers was due to a reduction in LK31C precursors from Gab2$^{-/-}$ mice. Unexpectedly, there was a slightly higher percentage of LK31C cells in Gab2$^{-/-}$ mice, which could reflect a compensatory mechanism (Fig. 6c). Hence, the reduction in CFU-C frequency likely reflects a defective ability of progenitors in the LK31C subset to respond to CSF-1.

CSF-1-responsive progenitors (LK31C) can be further distinguished on the basis of Flt3 expression. The LK31C subset was described as common myeloid progenitor-like (CMP-like) (57). Recent studies indicate that most cells of the granulocyte-macrophage (GM) lineage originate from Flt3$^+$ progenitors (2). Additionally, the Mφ and dendritic cell precursor (MDP) is Flt3$^+$ (1). LK31C cells could clearly be divided into two subsets based on Flt3 expression (Fig. 7a). LK31C cells showed low CSF-1R expression irrespective of Flt3 status, indicating they were more immature than MDPs. Also, LK31C could not unambiguously be classified as a CMP or GM progenitor (GMP) based on immunophenotyping (25). When cultured with CSF-1 as the only added cytokine, both Flt3$^+$ and Flt3$^-$ subsets increased CSF-1R expression (Fig. 7b). In methylcellulose containing SCF, IL-3, IL-6, and erythropoietin, the Flt3$^-$ subset from WT mice gave rise to more heterogeneous and primitive colonies, whereas the Flt3$^+$ subset was more exclusively granulocytes and Mφs. Thus, the CMP-like features previously mentioned likely originated from the Flt3$^-$ subset, whereas the Flt3$^+$ subset was more GMP-like. Minor differences were observed in colony formation in the presence or absence of Gab2 (Fig. 7c). The CFU-C frequency in the LK31C Flt3$^+$ subset was 1 in 10, the highest of any population we had examined, and WT LK31C Flt3$^+$ cells gave rise to 10-fold more CFU-C than those from Gab2$^{-/-}$ mice (Fig. 7d). We conclude that Gab2's impact on myeloid cell development is most pronounced in the CSF-1-dependent MNP lineage.

Gab2 is needed for CSF-1-dependent MNP progenitor proliferation and survival. We used CFSE to continuously track proliferation during CSF-1-induced differentiation (Fig. 8). BM cells labeled on D0 were stained with anti-CD31 to identify progenitors. CFSE dilution after 3 days was 1.5-fold greater in WT than Gab2$^{-/-}$ cells (Fig. 8a). D2 BM cells were similarly labeled with CFSE and stained with anti-CD11b to identify myeloid cells. CFSE dilution after 3 days was also

ment. High-side-scatter (SSC^{hi}) eosinophils, which also express F4/80 (58), were excluded as shown. (c) BM cells were stained with anti-CSF-1R. The percentage of CSF-1R$^+$ cells in individual mice is plotted. (d) Total BM cells were plated in methylcellulose in the presence of CSF-1 and scored on D7. Photomicrographs of D10 colonies are shown. (e) D2 cells were seeded and scored on D7. D10 colonies are shown, and Wright-Giemsa staining was performed on cytospins prepared from the colonies. A single WT CFU-C was used per cytospin, whereas all visible Gab2$^{-/-}$ CFU-C were pooled. In panels c and d, $n = 3$, with at least 5 mice/genotype.

a

Gab2+/+ D2 cells   Gab2-/- D2 cells

(i) CD31^loLy6C^-   (ii) CD31^highLy6C^-   (iii) CD31^+Ly6C^+

(iv) CD31^-Ly6C^+   (v) CD31^-Ly6C^high   x 600

b

+/+   -/-

D0: 14.1 / 9.21   12.3 / 8.53
D1: 24.7 / 0.4   12.5 / 1.99
D2: 31.5 / 0.92   13.2 / 9.31
D5: 45   26.1
D7: 14.6   5.58

c

Cell numbers in the indicated subset as a percent of cells seeded

p=0.004, p=0.006, p=0.0001, p=0.0001

D2 CD31+Ly6C+, D3 CD31+Ly6C+, D2 CD31-Ly6Chi, D3 CD31-Ly6Chi

■ Gab2+/+   ■ Gab2-/-

d

+/+   -/-
D2
40.6 / 1.6   23.1 / 8.7

CD31+CD11b+ (%)   CD31-CD11bhi (%)
days in culture

■ Gab2+/+, 2 mice   ● Gab2-/-, 2 mice

e

Gab2+/+ LIN*-   Gab2-/- LIN*-
(ii) 27.2 (iii) 40.2 (v) 8.07 (vi) 11.4   (ii) 16.2 24 (v) 39.8 (vi) 9.74

LIN*- subsets	Gab2+/+	Gab2-/-
CD31^highLy6C^- (ii)	28.3 ± 6.3	18.6 ± 2.2 *
CD31^+Ly6C^+ (iii)	42.4 ± 3.7	28.6 ± 3.1 **
CD31^-Ly6C^high (v)	10.7 ± 3.5	32.6 ± 6.1 **
CD31^-Ly6C^+ (vi)	13.0 ± 5.5	10.7 ± 3.5

n=4

f

LIN*-CD31^highLy6C^-   LIN*-CD31^+Ly6C^+
R0   R1   R2
CSF-1R   CSF-1R

Percent CSF-1R+
n=3
■ Gab2+/+   ■ Gab2-/-
CD31^highLy6C^-   CD31^+Ly6C^+

g

+/+   -/-   x 600
LIN*-CD31^highLy6C^-

CFU-C	Gab2+/+	Gab2-/-
LIN*-CD31^highLy6C^-	85 ± 4	23 ± 0.7

3000 cells plated, n=2, p=0.02

CD31   Ly6C

CD31+Ly6C+ (%)   CD31-Ly6Chi (%)
days in culture

■ Gab2+/+, 7 mice   ● Gab2-/-, 5 mice

2-fold greater for WT cells (Fig. 8b). These data indicate that WT BM cells proliferated to a greater extent than Gab2$^{-/-}$ cells throughout *ex vivo* culture in CSF-1. To verify that the reduction in CFSE dilution in Gab2$^{-/-}$ cells accurately reflected what was happening in CSF-1-responsive progenitors, we sorted for LIN*$^-$ CD31^{high} Ly6C$^-$ cells. Compared to cells from WT mice, those from Gab2$^{-/-}$ mice had 2-fold more annexin$^+$ cells and 2-fold fewer BrdU$^+$ cells (Fig. 8c). Next, we purified LK31C cells and cultured them in CSF-1 (Fig. 8d). Based on scatter, more LK31C Gab2$^{-/-}$ cells died during differentiation, compared to WT cells. CFSE dilution on D2 and D4 in WT cells was greater than that of Gab2$^{-/-}$ cells, showing a higher proliferative rate in WT BM progenitors. By D7, enough divisions had occurred in both WT and Gab2$^{-/-}$ cells that CFSE was no longer detected. Despite the difference in CFU-C frequencies (Fig. 7d), both Flt3$^+$ and Flt3$^-$ subsets expanded (60- and 47-fold) over 7 days in liquid culture (Fig. 8e), indicating that CSF-1 had a strong selective influence over early progenitors. Additionally, for both LK31C subsets, at D7, Gab2$^{-/-}$ cultures had 3- to 4-fold fewer cells than the WT. Thus, although the difference in CFU-C numbers between the WT and Gab2$^{-/-}$ LK31C Flt3$^-$ subsets was less than that for the LK31C Flt3$^+$ subsets (Fig. 7d), Gab2$^{-/-}$ LK31C Flt3$^-$ progenitors still produced fewer Mϕs. These results show that Gab2 is required for optimal CSF-1-mediated survival and proliferation of BM progenitors.

Reexpression of WT Gab2 in Gab2$^{-/-}$ BM cells rescues CFU-C number and size. To confirm that Gab2 deficiency is the cause of defective CFU-C formation, we transduced BM cells with a WT Gab2-expressing retrovirus (Fig. 9a and b). Reintroduction of WT Gab2 to Gab2$^{-/-}$ BM increased CFU-C numbers by 7-fold and restored colony size (Fig. 9b to d). No major difference was observed between WT cells transduced with empty or WT Gab2 virus, ruling out a nonspecific effect. These data verify that Gab2 is required for maximal production of CFU-C and their proliferation.

Gab2 utilizes PI3K and SHP2 to maximally promote CFU-C formation. To identify the pathways Gab2 uses to promote MNP expansion, we transduced BM cells with 3YF-Gab2 that lacks PI3K binding sites (Fig. 9a). 3YF-Gab2 suppressed CFU-C formation in WT cells, and the colonies were much smaller (Fig. 9b to d), suggesting a dominant-negative effect (36). In Gab2$^{-/-}$ cells, 3YF Gab2 only partially restored CFU-C number and size compared to WT Gab2 (Fig. 9c and d). While supporting the importance of the Gab2-PI3K path-

way, these data also implicate an additional pathway(s) downstream of Gab2. The difference between WT and 3YF Gab2 is not because of marked differential expression of these proteins since transduction efficiencies and GFP expression were similar (e.g., the MFI was 247 versus 232 for Gab2$^{-/-}$ BM cells transduced with WT and 3YF Gab2, respectively). Although 3YF Gab2 in BMMs differentiated from transduced progenitors was present at ≈50% the level of WT Gab2, CFU-C generation is more likely to be dependent on the level of Gab2 in progenitors (Fig. 9g). Constitutively active Akt (E40K Akt) (28, 36) substantially rescued CFU-C number, although not as effectively as WT Gab2. However, the size of E40K-transduced CFU-C was comparable to that of CFU-C transduced with WT Gab2. Exogenous expression of 3YF Gab2 or E40K did not perturb the ability of CFU-C to differentiate to Mϕs (Fig. 9d). PI3K inhibition with LY294002 (LY) suppressed CFU-C formation in WT cells transduced with the empty vector control and in Gab2$^{-/-}$ cells transduced with WT Gab2 (Fig. 9e), supporting the importance of the PI3K-Akt pathway in CFU-C formation. To identify the second pathway that Gab2 uses to promote CFU-C formation, we examined Gab2 recruitment of SHP2. Similar to 3YF-Gab2, expression of DM-Gab2 lacking SHP2 binding sites in Gab2$^{-/-}$ cells modestly increased colony number (Fig. 9f) and size (not shown). Thus, Gab2 depends on both PI3K and SHP2 to support CSF-1-dependent CFU-C expansion.

Phospho-flow analysis reveals defective Akt, Erk, and S6 signaling in Gab2$^{-/-}$ CD31^{high} Ly6C$^-$ progenitors. To determine directly how Gab2 impacts the CSF-1 signaling pathways in the CD31 and Ly6C subsets, we used flow cytometry (26, 40). We analyzed the LIN*$^-$ population rather than LK31C cells because phospho-flow analysis required significant numbers of cells; also they have low CSF-1R levels, and the assay may not be sufficiently sensitive to detect a signal. Our protocol preserved the CD31 and Ly6C subsets seen with live cell staining (compare Fig. 10a and 5d). CD31$^-$ Ly6C$^+$ cells that should not respond to CSF-1 were used as a negative control, and CD31$^-$ Ly6C^{high} MOs that should be activated by CSF-1 were used as a positive control. CSF-1R staining was not compatible with the phospho-flow protocol, so we used scatter to gate on the CSF-1R$^+$ population in LIN*$^-$ CD31$^+$ Ly6C$^+$ cells (LIN*$^-$ CD31$^+$ Ly6C$^+$ R2). We gated on the entire LIN*$^-$ CD31^{high} Ly6C$^-$ subset since scatter did not reveal distinct subpopulations (Fig. 5e).

CSF-1 induced a clear phospho-Akt signal in the LIN*$^-$

FIG. 5. Gab2 deletion is associated with decreased CD31^{high} Ly6C$^-$ and CD31$^+$ Ly6C$^+$ cell numbers during *in vitro* MNP differentiation. (a) D2 cells were flow sorted into CD31 and Ly6C subsets. Cytospins stained with Wright-Giemsa revealed CD31^{lo} Ly6C$^-$ lymphocytes (i), CD31^{high} Ly6C$^-$ blasts (ii), CD31$^-$ Ly6C$^+$ granulocytes (iv), and CD31$^-$ Ly6C^{high} MOs (v). The CD31$^+$ Ly6C$^+$ subset (iii) is a mixture of blasts, monoblasts, MOs, and Mϕs. The CD31$^-$ Ly6C^{high} subset was from Gab2$^{-/-}$ cells. (b to d) Total BM cells were differentiated for 7 days and analyzed by FACS. (b) CD31$^+$ Ly6C$^+$ and CD31$^-$ Ly6C^{high} gates are shown for D0 to D2, and the CD31$^-$ Ly6C^{high} gate is shown for D5 to D7. Data were averaged from individual mice. (c) The data in panel b are shown as a percentage of the number of cells seeded 24 h prior to analysis (*x*), calculated by multiplying the percentage in the indicated subset by the total cell number present in the culture and dividing by *x*. The normalization accounted for the small differences in cell numbers seeded between experiments. (d) CD31$^+$ CD11b$^+$ gates are shown and data presented as in panel b. (e) D2 cells were lineage depleted to generate LIN*$^-$ cells. Shown are representative CD31 and Ly6C plots of LIN*$^-$ cells. The LIN*$^-$ CD31$^-$ Ly6C$^+$ subset (vi) is Ly6G$^-$ and CSF-1R$^-$, indicating it is nonmonocytic and nongranulocytic. (e) Subsets from panel d were further gated on scatter. CSF-1R histograms are shown for the R0 gate in LIN*$^-$ CD31^{high} Ly6C$^-$ and the R2 gate in LIN*$^-$ CD31$^+$ Ly6C$^+$: FMO, thin black lines; WT, black lines; Gab2$^{-/-}$, gray lines; and R1, thin gray lines. CSF-1R expression in the LIN*$^-$ CD31 and Ly6C subsets is plotted as a percentage of all cells. (g) LIN*$^-$ CD31^{high} Ly6C$^-$ cells were sorted. Corresponding cytospins and CFU-C numbers are shown. Each experiment pooled cells from at least 3 mice of each genotype.
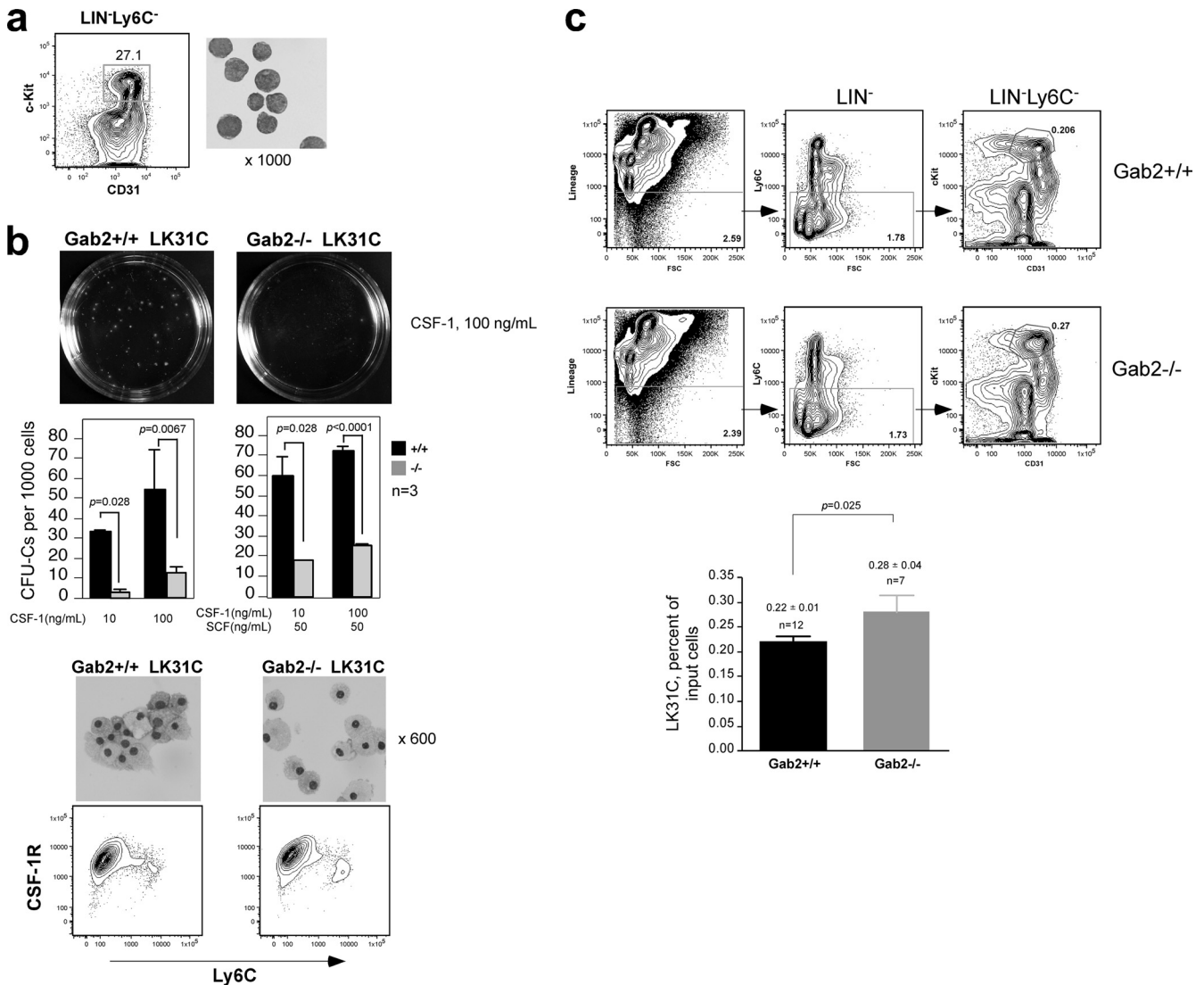
FIG. 6. Gab2 is required for optimal expansion of CSF-1-responsive colony-forming myeloid progenitors (LK31C). (a) Freshly isolated BM cells were lineage depleted and sorted for LIN⁻ c-Kit⁺ CD31^high Ly6C⁻ (LK31C) cells. Cytospins show blast-like morphology. (b) CFU-C in the presence of CSF-1 ± SCF. Each experiment used 3 mice per genotype. Cytospins from individual colonies were stained and analyzed by FACS. (c) Freshly isolated BM cells were stained with lineage antibodies and antibodies to Ly6C, c-Kit and CD31. The sequence indicated by arrows shows the hierarchical gating strategy. The LK31C fraction is shown as a percentage of total input cells. n, number of mice.

CD31^high Ly6C⁻ subset in WT cells which was abolished by LY, confirming the signal to be Akt (Fig. 10b). There were more WT cells responding to CSF-1, consistent with more CSF-1R⁺ cells (Fig. 5e). The intensity and duration of phospho-Akt signal were also enhanced in WT relative to −/− cells (Fig. 10b, inset), indicating that Gab2 is required for optimal Akt activation in the CD31^high Ly6C⁻ progenitors. Less of a difference was observed for LIN*⁻ CD31⁺ Ly6C⁺ R2 cells, and when the higher basal phosphorylation in WT cells was accounted for, the maximal fold increase was similar. This suggests that Gab2 is less important for Akt activation in the more mature precursors. CSF-1-induced phospho-Erk was also reduced in Gab2^−/− LIN*⁻ CD31^high Ly6C⁻ cells compared to WT cells, but less so in LIN*⁻ CD31⁺ Ly6C⁺ R2 cells when corrected for basal values (Fig. 10c). U0126 (U0) pretreatment confirmed that the signal was Erk. Phosphorylation of ribo-

somal protein S6 has been used as a readout for the PI3K pathway (70). The LIN*⁻ CD31^high Ly6C⁻ subset in Gab2^−/− cells showed a reduction in the fraction of responding cells and phospho-S6 intensity (Fig. 10d), while a smaller difference was observed between WT and Gab2^−/− LIN*⁻ CD31⁺ Ly6C⁺ R2 cells. LY only partially reduced phospho-S6, as did U0, but the combination completely eliminated CSF-1-induced phospho-S6 (Fig. 10d). Therefore, CSF-1-induced S6 phosphorylation is dependent on both the PI3K and Erk pathways. Although cells in the LIN*⁻ CD31^high Ly6C⁻ subset showed a range of CSF-1R expression levels (Fig. 5e), the phosphorylation histograms for Akt, S6, and Erk were essentially bimodal, with two distinguishable groups: CSF-1R⁺ cells that responded and CSF-1R⁻ cells that did not. As D2 Gab2^−/− cells have a higher percentage of MOs, their response would have obscured that from the progenitors had bulk cells been analyzed
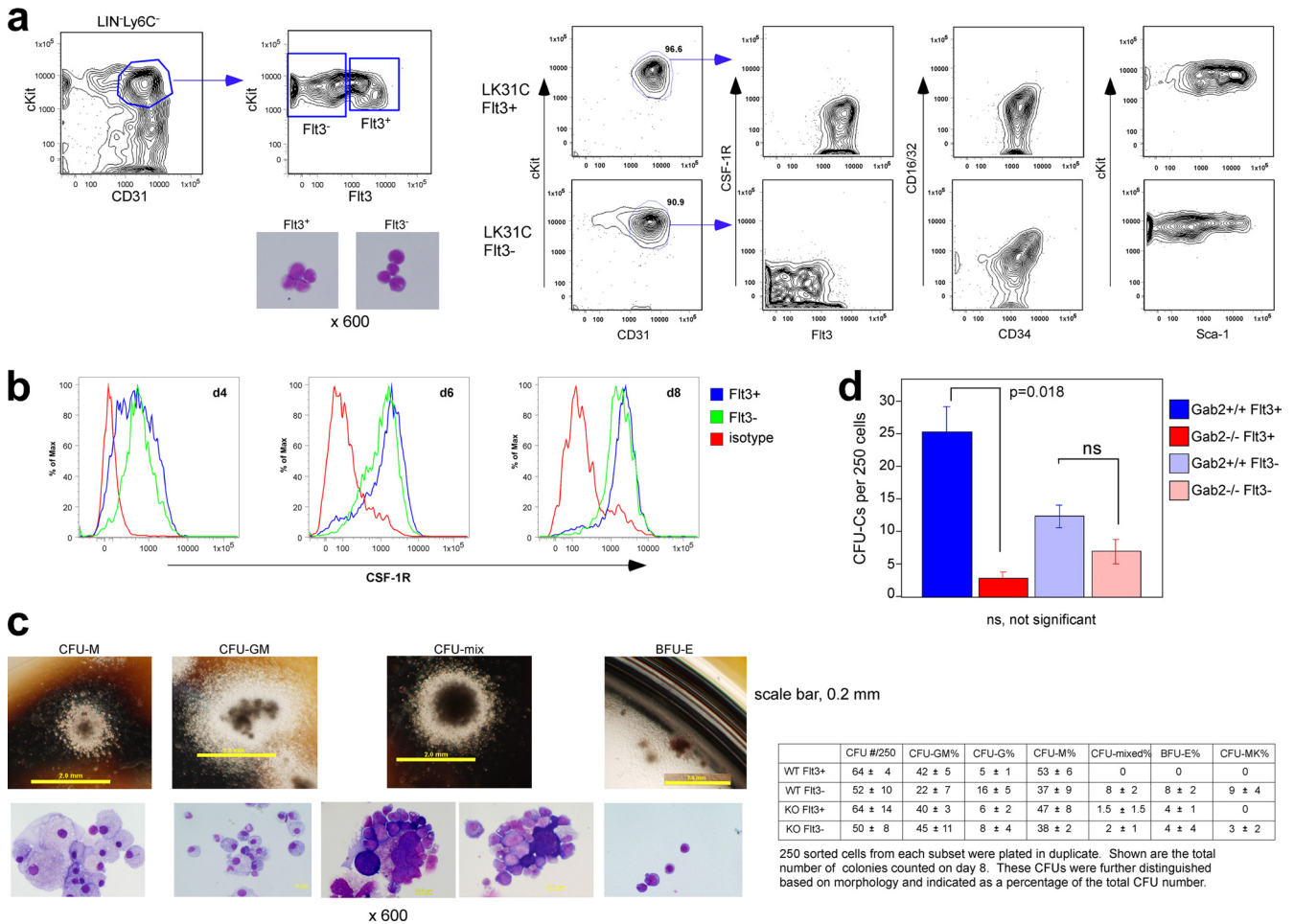
FIG. 7. LK31C Flt3$^+$ progenitors are enriched for CSF-1-responsive progenitors. (a) Immunophenotyping of LK31C Flt3$^+$ and Flt3$^-$ subsets. Shown are results representative of at least 3 independent experiments. (b) Sorted cells were cultured in CSF-1, and CSF-1R expression was determined by FACS. (c) Cells were plated in methylcellulose containing SCF, IL-3, IL-6, and erythropoietin (Epo). Representative colonies and their corresponding cytospins are represented as follows: CFU-M consists of exclusively Mϕs, CFU-GM contains Mϕs and granulocytes, CFU-mix contains Mϕs, erythroid cells, megakaryocytes, and cells of the granulocytic lineage, and BFU-E contains erythroid cells. (d) CFU-C assay. Panels c and d show the results from 4 (WT) or 2 (Gab2$^{-/-}$) independent experiments; each experiment pooled cells from 5 mice/genotype.

by immunoblotting. We conclude that in MNP precursors, Gab2 is necessary for optimal CSF-1 signaling to the PI3K and Erk pathways.

Gab2 is needed for optimal proliferation of BMMs. We next examined the role of Gab2 in mediating MNP proliferation during the later stages of differentiation. Gab2$^{-/-}$ BMMs showed lower CSF-1-induced cell number increases (Fig. 11a). In agreement, continuously growing BMMs had twice as many WT cells in S plus G$_2$/M compared to Gab2$^{-/-}$ cells (Fig. 11b). Differences in viability were not detected (not shown). MTS analysis confirmed the growth defect of Gab2$^{-/-}$ BMMs (Fig. 11c). When WT Gab2 was overexpressed in D5 cells, the mitogenic defect of Gab2$^{-/-}$ BMMs was completely rescued, verifying that late-stage MNPs also required Gab2 for maximal proliferation independent of Gab2's role in early BM progenitors.

Signaling in BMMs. Gab2 deficiency did not change CSF-1R activity in BMMs as assessed by phosphorylation of the activation loop tyrosine (Fig. 11d). In contrast to BM progenitors, CSF-1-provoked phosphorylation of Akt and S6

was essentially normal in Gab2$^{-/-}$ BMMs, as was that of Stat3/5. At earlier times, S6 phosphorylation was higher in Gab2$^{-/-}$ cells; however, the significance of this is unclear as phosphorylation at these time points was 4- to 5-fold lower than peak values. Expression of Gab1 and Gab3 was increased in Gab2$^{-/-}$ BMMs (Fig. 11e) and may explain why Akt and S6 phosphorylation was maintained in these cells. Gab2 deficiency, however, increased phosphorylation of Erk and JNK but not p38 (Fig. 11f). Consistent with previous results (49), CSF-1 activated JNK1 and not JNK2. BMMs deprived of CSF-1 for 21 h showed elevated levels of phospho-JNK that was suppressed in the presence of CSF-1 in WT BMMs but partially in Gab2$^{-/-}$ cells, confirming deregulation of the CSF-1-dependent JNK pathway in the absence of Gab2 (Fig. 11g). In contrast, LPS, a potent stimulator of JNK activity in BMMs, activated JNK1/2, and JNK phosphorylation was not altered by the absence of Gab2 (Fig. 11h). Although persistent CSF-1-induced Erk activity can lead to cell cycle arrest (30), inhibition of Erk activity resulted in diminished proliferation in both WT and Gab2$^{-/-}$ BMMs (Fig. 11i). We therefore focused on de-
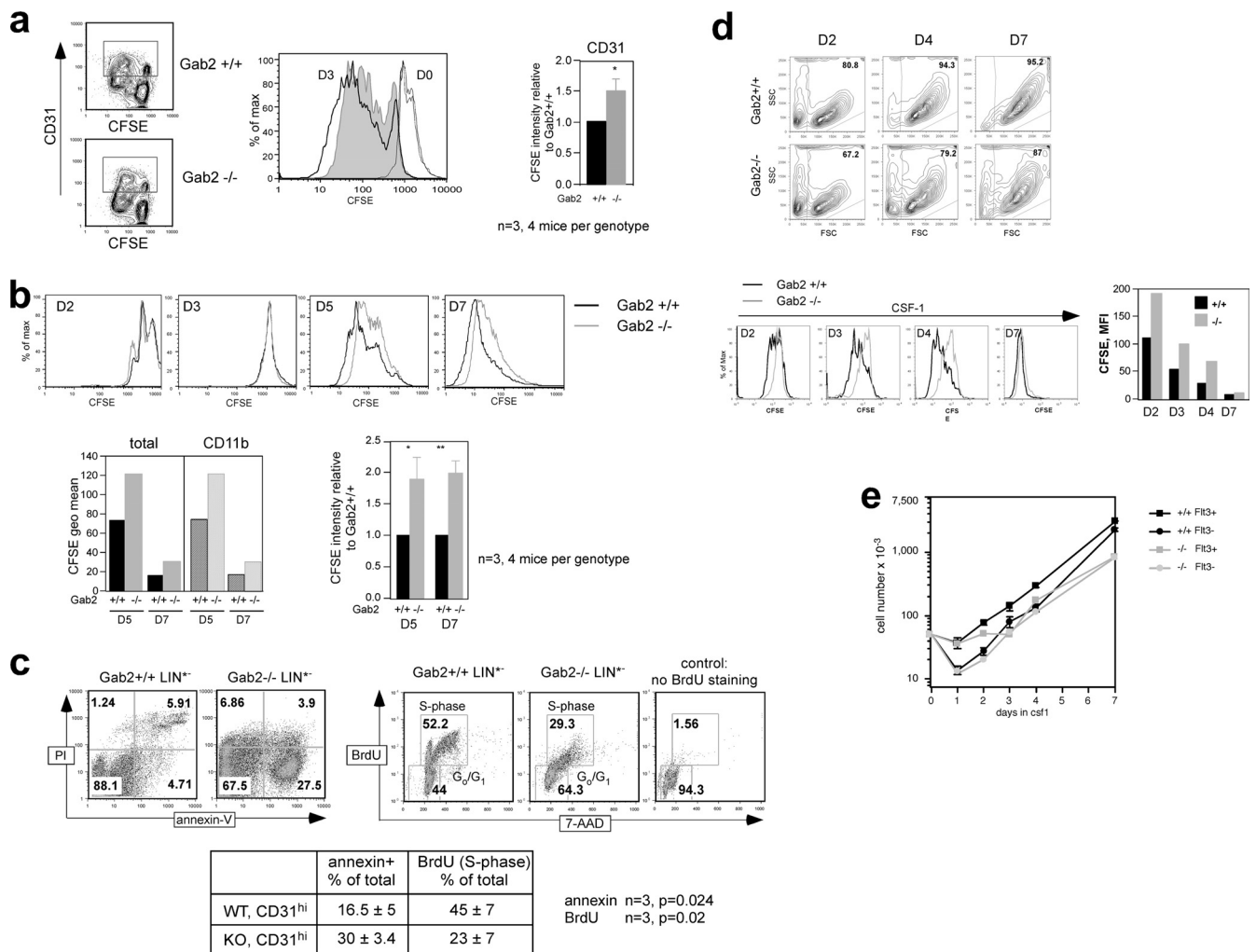
FIG. 8. Impaired CSF-1-dependent proliferation and survival during MNP development in Gab2$^{-/-}$ bone marrow. (a) Total BM cells were labeled with CFSE and either immediately processed (D0) or differentiated for 3 days. Gating was on the CD31$^+$ subset. D0, both genotypes (thin black lines); D3, WT (black lines); D3, Gab2$^{-/-}$ (gray shading). Corresponding geometric mean fluorescence intensities (MFI) are plotted. (b) D2 cells were labeled with CFSE and either immediately processed (D2) or differentiated. CFSE histograms are shown with representative plots of MFIs on D5 and D7 in the total and CD11b$^+$ gates. The averaged MFIs in the total gate were normalized to WT. (c) Sorted LIN*$^-$ CD31^{high} Ly6C$^-$ cells were cultured in CSF-1 and analyzed for apoptosis and BrdU incorporation in the CD11b$^+$ gate. (d) LK31C cells were immediately labeled after sorting with CFSE and cultured in CSF-1. Scatter plots, CFSE histograms, and the corresponding MFIs are shown. (e) A total of 5 × 10^4 LK31C Flt3$^+$ and Flt3$^-$ cells were cultured in CSF-1, and cell counting was performed in duplicate (results from 1 of 2 experiments are shown).

regulated JNK1 activity as a possible cause of reduced proliferation in Gab2$^{-/-}$ BMMs. We asked if the increase in JNK1 activity is at the level of JNK kinases (JNKKs) MKK4 and MKK7 (6). In BMMs, we could only detect CSF-1-induced phosphorylation of MKK7 and not MKK4, but MKK7 phosphorylation was not affected by Gab2 deficiency (Fig. 11j). Since JNK activity is also regulated by dually specific phosphatases (DUSPs), several of which are inducible at the transcriptional level (39), we examined the effect of the transcriptional inhibitor actinomycin D (AD). AD pretreatment did not alter acute CSF-1-induced JNK phosphorylation but increased phosphorylation in WT but not Gab2$^{-/-}$ cells after 2 h (Fig. 11j), consistent with a role for inducible JNK phosphatases in the sustained phase of JNK phosphorylation in Gab2$^{-/-}$ cells. Taken together, our data reveal that depending on develop-

mental stage, Gab2 may impact different signaling pathways in cells of the MNP lineage.

Downregulating JNK signaling or expression in Gab2$^{-/-}$ BMMs restores proliferation. We inhibited JNK signaling using a peptide derived from the JNK-binding motif of JIP (3) (JNKI-1). JNKI-1 treatment rescued CSF-1-dependent proliferation in Gab2$^{-/-}$ BMMs but had little effect in WT cells (Fig. 11i). We confirmed this observation by lentiviral delivery of specific shRNAs against JNK1 (Fig. 11k). shJNK1-1 to -4 decreased JNK1 protein levels by 80, 33 to 36, 68 to 69, and 53 to 57%, respectively. The almost complete elimination of JNK1 by shJNK1-1 and shJNK1-3 had a deleterious effect on CSF-1-dependent proliferation in WT and Gab2$^{-/-}$ BMMs. In contrast, a modest reduction of JNK1 levels by shJNK1-2 had a minimal effect on WT cells but restored proliferation almost
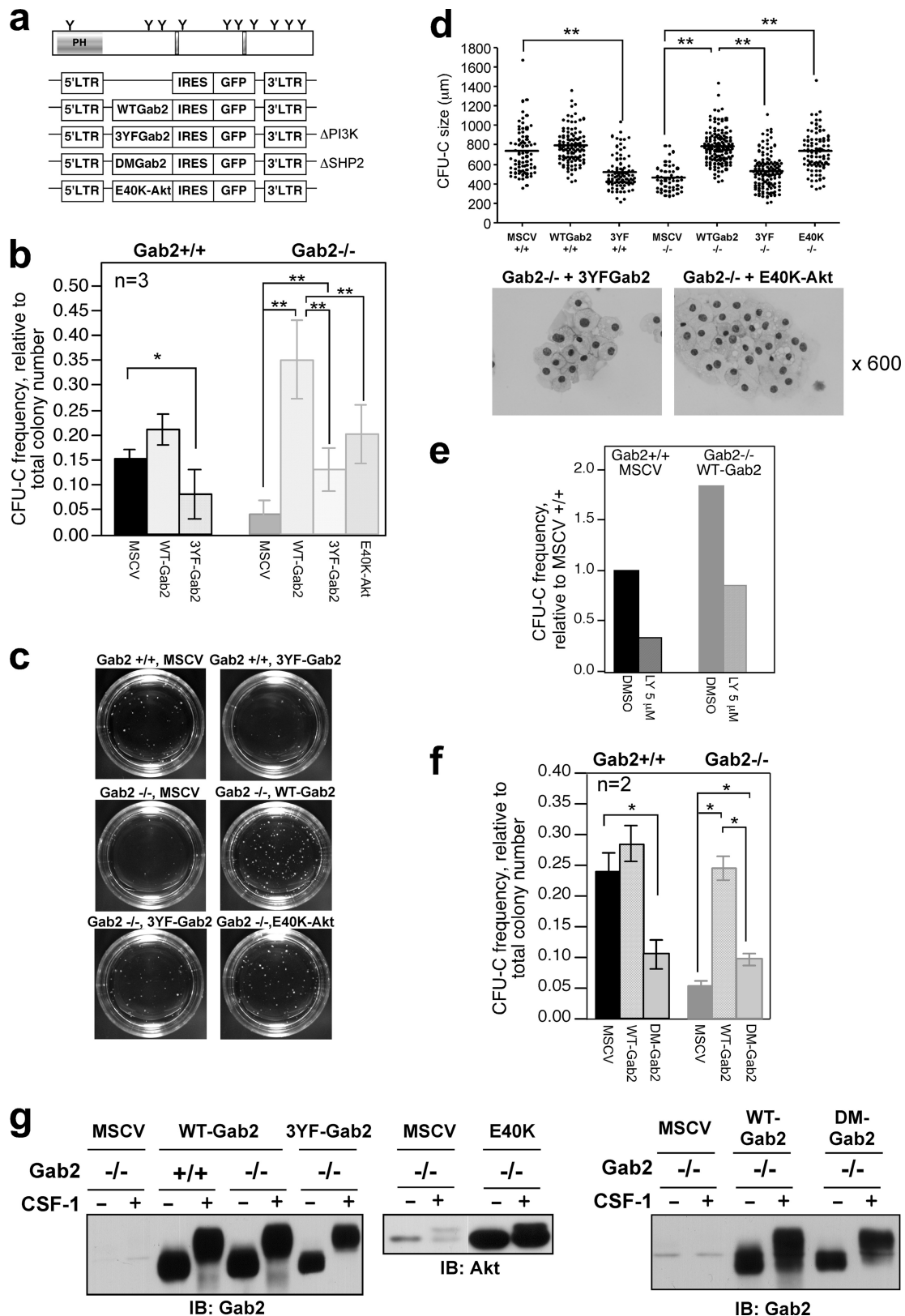
FIG. 9. Reexpression of WT Gab2 in Gab2$^{-/-}$ BM progenitors completely rescues CFU-C formation, while Gab2 mutants deficient in PI3K or SHP2 recruitment are partially effective. (a) Murine stem cell virus (MSCV; empty vector control)-internal ribosome entry site (IRES)-enhanced green fluorescent protein (EGFP) retroviral constructs. LTR, long terminal repeat. (b) CFU-C assay of sorted GFP$^+$ cells. CFU-C frequency is relative to total colony number from each experiment. (c) Photomicrographs of CFU-C. (d) CFU-C size and Wright-Giemsa stains of cytospins from CFU-C transduced with the indicated viruses. (b to d) Data were from 3 independent experiments. (e) CFU-C assay of WT and Gab2$^{-/-}$ BM cells transduced with empty vector or WT Gab2, respectively, with or without LY294002 (LY). (f) CFU-C assay of sorted GFP$^+$ cells. (g) Sorted cells were differentiated in liquid culture for 7 days, and Gab2 and Akt levels in BMMs were determined.
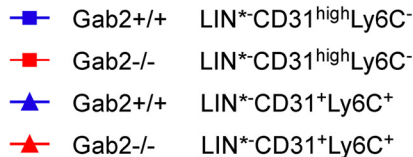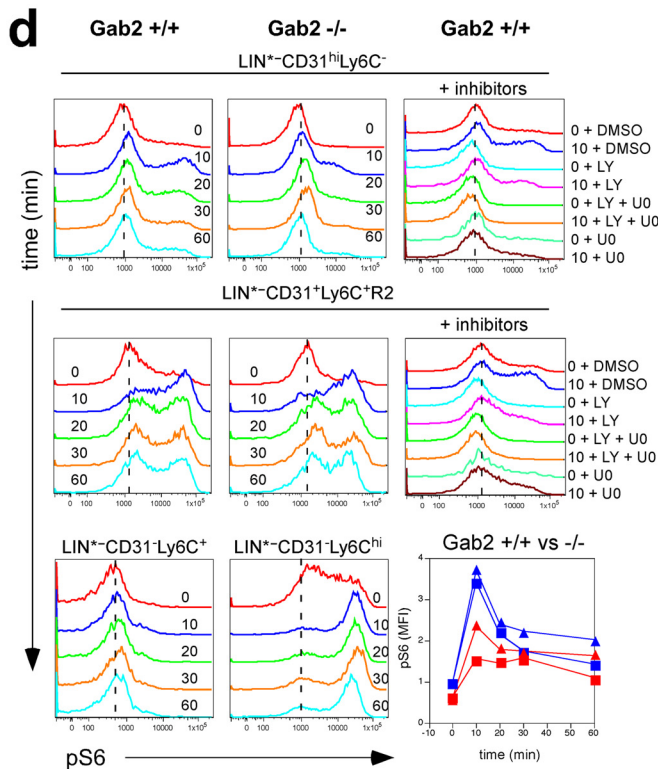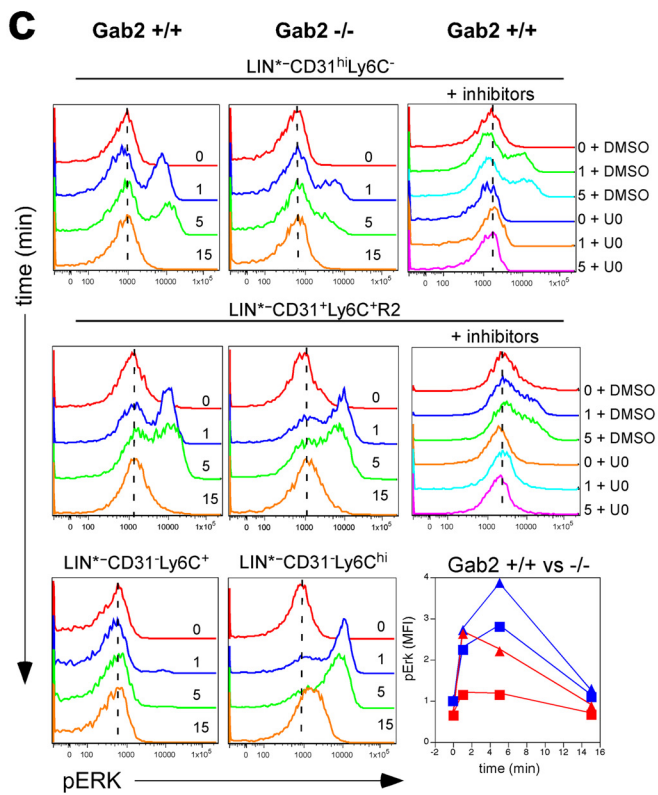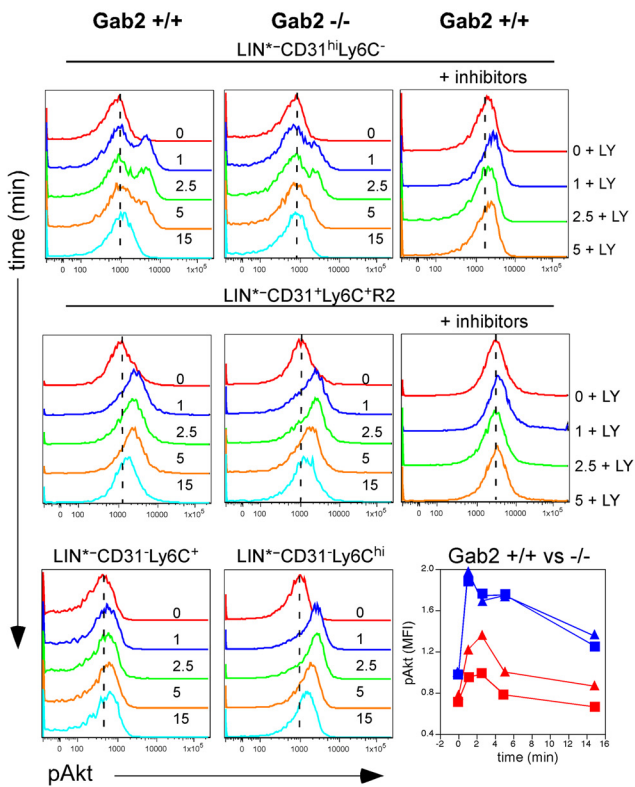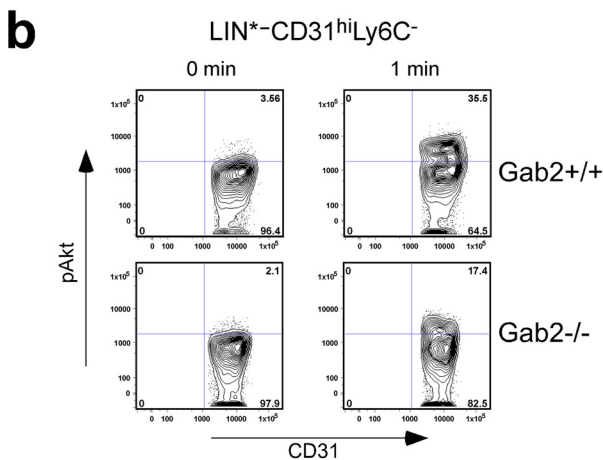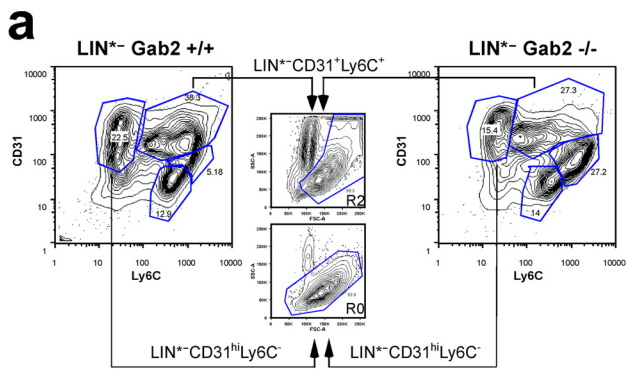
completely to Gab2$^{-/-}$ cells; the effect of shJNK1-4 was intermediate. Altogether, our findings support the hypothesis that an optimal level of JNK1 activity is required for cellular proliferation.

Fewer MOs or Mφs are recruited to the peritoneum in Gab2$^{-/-}$ mice in a sterile peritonitis model. Since Gab2$^{-/-}$ mice have a significant defect in CSF-1-dependent MNP development, we asked if this deficit could be exacerbated under inflammatory conditions. In the absence of inflammation, only a trend toward decreased peritoneal MO or Mφ numbers was observed in Gab2$^{-/-}$ mice: WT, $(2.0 \pm 0.3) \times 10^6$ ($n = 7$); Gab2$^{-/-}$, $(1.6 \pm 0.3) \times 10^6$ ($n = 6$). Within 24 h of thioglycolate (TG) injection, WT mice had mounted a robust peritoneal response. We recovered fewer peritoneal cells from Gab2$^{-/-}$ mice, and the reduction in MO or Mφ numbers was even more significant (Fig. 12a). Since the difference in percentages of MOs or Mφs in total cells was smaller between WT and Gab2$^{-/-}$ cells (Fig. 12a) compared to the difference in total cells (4.02×10^7 versus 1.99×10^7 at 72 h), the major source of the difference appeared to be fewer MNPs arriving at the peritoneum of Gab2$^{-/-}$ mice. We assessed the BM response by determining the number of CFU-C in BM at the time of sacrifice (Fig. 12b). CFU-C numbers increased by 70% at 24 h in WT mice compared to a 28% increase in Gab2$^{-/-}$ mice. A similar reduction in CFU-C numbers was observed when mice were challenged with LPS (Fig. 11c). Therefore, Gab2$^{-/-}$ mice are significantly less able to elicit an MNP response to an inflammatory challenge, in part due to a defective bone marrow response.

DISCUSSION

Using a myeloid cell line and Gab2 nullizygous mice, we identified Gab2 as an essential mediator throughout CSF-1-dependent MNP development. We detected the highest frequency of CSF-1-responsive early progenitors in the LIN$^-$ cKit$^+$ CD31^{high} Ly6C$^-$ Flt3$^+$ subset. CD31^{high} Ly6C$^-$ progenitors but not BMMs depend on Gab2 to maximally activate Akt, Erk, and S6, corroborated by the requirement for Gab2 interactions with PI3K and SHP2 to maximally promote CFU-C expansion. Unexpectedly, Gab2$^{-/-}$ BMMs show enhanced Erk and JNK1 phosphorylation, but only deregulated JNK1 activity was linked to diminished CSF-1-dependent proliferation. Of note, the defective CSF-1 response in Gab2$^{-/-}$ BM cells *in vitro* correlated with fewer F4/80$^+$ MOs or Mφs in the resident BM and a reduced ability to increase CFU-C production in response to inflammatory challenges *in vivo*.

Each Gab gene has been deleted in the mouse. Gab1's role in the myeloid lineage is unknown, whereas Gab3 deletion has no effect on hematopoiesis (51). A study examining the combined effects of early acting cytokines in Gab2$^{-/-}$ mice noted a reduction in colony-forming activity (70). By focusing on the MNP lineage, we uncovered an essential requirement for Gab2 in CSF-1-dependent MNP development. The earliest cell that can respond to CSF-1 alone is the CFU-C (52), which Leenen suggested to reside in the CD31^{high} Ly6C$^-$ population (11). Two days after differentiation induction, BM cells from Gab2$^{-/-}$ mice generated significantly fewer CSF-1R$^+$ CD31^{high} Ly6C$^-$ early progenitors and CSF-1R$^+$ CD31$^+$ Ly6C$^+$ late-stage MNP precursors compared to WT mice. Additionally, purified LIN^{*-} CD31^{high} Ly6C$^-$ and LK31C progenitors showed diminished proliferation and survival during culture in CSF-1. Hence, the net reduction in the percentage of F4/80$^+$ MOs and Mφs in Gab2$^{-/-}$ mice is explained by the diminished cell intrinsic capacity for progenitor expansion. Osteopetrosis in Gab2$^{-/-}$ mice (24, 61) results in a smaller marrow cavity and reduced total cellularity, so that the absolute numbers of MOs and Mφs in the BM are further decreased. A study using a different Gab2$^{-/-}$ line reported no difference in BM cellularity and speculated that the discrepancy might be due to the difference in targeting strategy employed to generate the Gab2$^{-/-}$ mice used in the present work (70). We found no evidence to support the existence of a mutant Gab2 protein since published immunoblots (61) and those in this study showed the absence of any Gab2 protein in the 100- to 25-kDa range in Gab2$^{-/-}$ BM-derived cells.

The premature appearance of MOs in Gab2$^{-/-}$ cultures suggests that accelerated differentiation could also contribute to diminished proliferation. An inverse correlation between proliferation and differentiation has been noted for stem cells; for example, Notch signaling enhances self-renewal, while its inhibition promotes differentiation (12). CSF-1 couples proliferation and differentiation, and possibly the primary defect in the absence of Gab2 is enhanced differentiation, with decreased proliferation as a secondary effect. Our data from 32D.R, a cell line that proliferates but does not differentiate in response to CSF-1, support the notion that Gab2 has a direct effect on proliferation. Earlier studies with the FDC-P1 cell line reported that Gab2 mediates Mφ differentiation (33). Our data here show the opposite—that Gab2's main role in primary myeloid cells is to promote proliferation and survival and in Gab2's absence, accelerated not defective differentiation is observed, underscoring the importance of studying differentiation in the proper cellular context.

Fate-mapping studies demonstrate that cells in the GM lineage pass through an Flt3$^+$ progenitor stage (2). We discovered that LK31C progenitors could be further discriminated based on Flt3 expression. While a combination of IL-3, CSF-1, and IL-1 was previously used (57), we added only CSF-1 and found that both Flt3$^+$ and Flt3$^-$ subsets proliferated and differentiated to Mφs despite minimal surface CSF-1R expression. This observation supports the existence of early myeloid progenitors in the LK31C subset capable of responding to CSF-1 alone. Elucidating the relationship of LK31C progeni-

FIG. 10. Gab2 deficiency reduces Akt, Erk, and S6 phosphorylation in CSF-1-responsive BM progenitors. (a) LIN^{*-} CD31 and Ly6C subsets used in phospho-flow analysis. The LIN^{*-} CD31$^+$ Ly6C$^+$ subset was further segregated based on scatter (see text). Panels b to d show phospho histograms for the indicated subset at each time point (min) after CSF-1 addition. Inhibition by 20 μM LY and inhibition by 10 μM U0126 (U0) were used as controls for pAkt and pErk, respectively. Also included as controls are LIN^{*-} CD31$^-$ Ly6C$^+$ cells (WT or Gab2$^{-/-}$), which do not respond to CSF-1, and LIN^{*-} CD31$^-$ Ly6C^{high} MOs (Gab2$^{-/-}$), which do respond. DMSO, dimethyl sulfoxide. The inset shows a plot of MFIs normalized to the WT signal at time 0. Data are representative of at least 3 independent experiments.
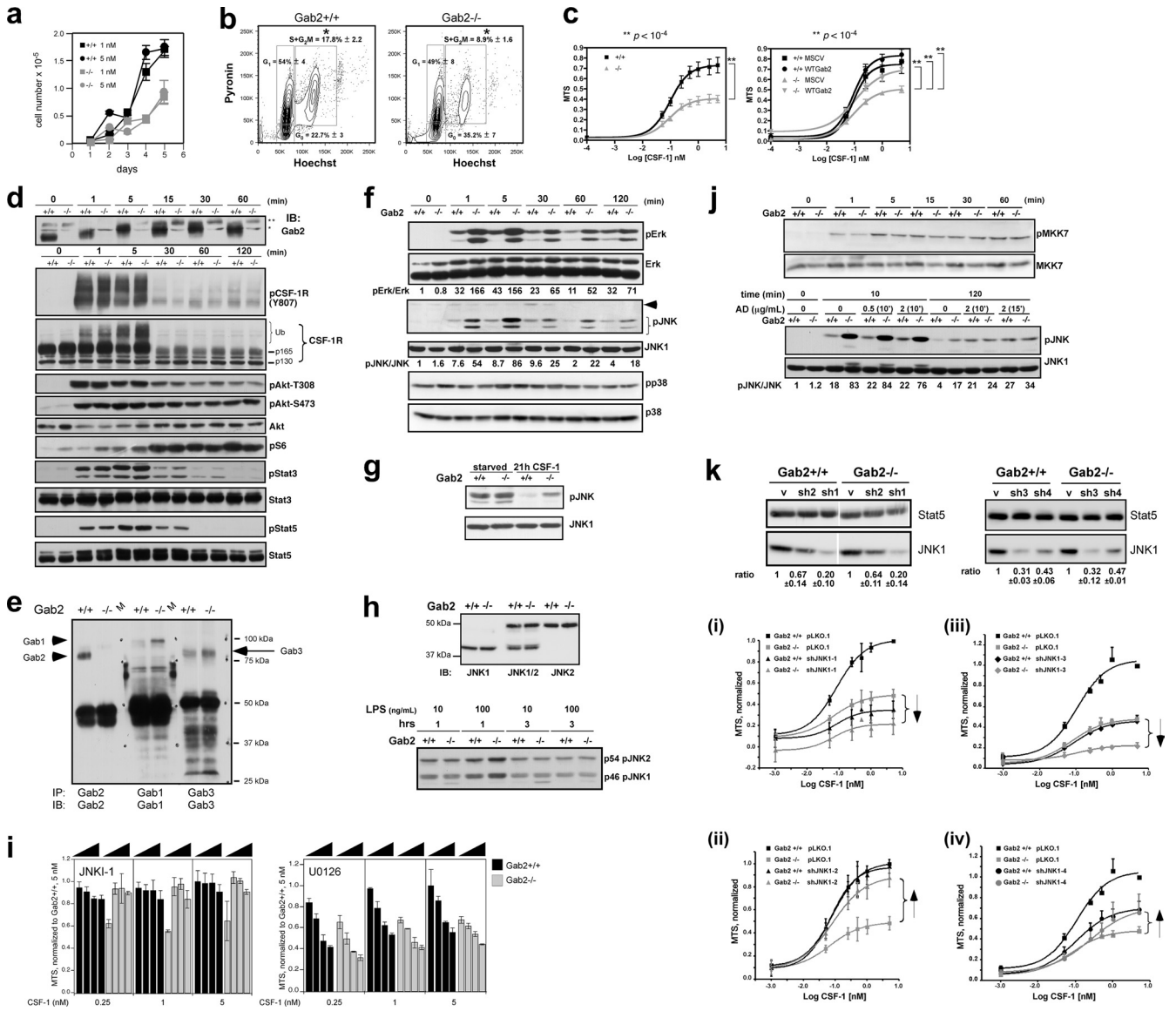
FIG. 11. Gab2 deficiency increases CSF-1-induced JNK phosphorylation and reduces CSF-1-dependent proliferation in late-stage MNPs. (a) D5 BMMs were plated in CSF-1, and all cells were counted. The differences between WT and −/− cells are all significant. (b) D7 BMMs were stained with Hoechst 33258 and pyronin Y. Three independent experiments were performed. (c, left) D5 cells were seeded in 96-well plates and assayed after 48 h for MTS reduction. Four experiments were performed, each using cells from at least 2 mice/genotype. (Right) D5 cells were transduced with empty (MSCV) or WT Gab2 retrovirus. GFP+ cells were sorted and plated. Three transductions were performed. (d) Immunoblot analysis of BMMs stimulated with CSF-1. ∗, nonspecific band; ∗∗, probably cross-reacting Gab1 band. (e) Gab levels in D7 BMMs. M, molecular mass markers (kDa). (f) Mitogen-activated protein kinase (MAPK) phosphorylation in BMMs. The position of pJNK corresponds to p46 JNK1. The pJNK doublet has been noted previously (60). An arrowhead indicates the position of p54 JNK2. Shown are representative data from at least 3 independent experiments. (g) BMMs were deprived of CSF-1 (starved) or cultured in CSF-1 for 21 h. (h, top) BMMs were blotted with antibodies that specifically recognized JNK1, JNK1 and JNK2, or JNK2. (Bottom) BMMs were stimulated with LPS, and pJNK immunoblotting was performed. (i) MTS analysis of BMMs: L-JNKI-1, 0, 0.5, 1, or 2 μM; U0126, 0, 1, 5, or 10 μM. (j, top) Phospho-MKK7 immunoblot of BMMs. (Bottom) BMMs were pretreated with 0.5 or 2 μg/ml of actinomycin D for 10 or 15 min before CSF-1 addition. (k) Knockdown of JNK1 in BMMs. (Top) JNK1 levels in cells transduced with empty vector (v), shRNA-JNK viruses (sh1 to -4), with Stat5 levels as loading control. Quantification was based on 2 experiments (mean ± SD). (Bottom) MTS analysis of transduced BMMs. Shown are the results from 3 (i and ii), 4 (iii), or 5 (iv) separate transductions. Each experiment was performed in triplicate and with values expressed relative to the maximum value in WT cells transduced with empty virus.

tors to other myeloid progenitors will have to await lineage tracing experiments, e.g., with *Cx3cr1gfp/+* (1) or Mac-Green (50) mice. CSF-1 may have an instructive role in lineage commitment in hematopoietic stem cells (HSCs) and GMPs (53). Our studies did not specifically address this question, although

we observed some cell death during differentiation especially for Gab2−/− cells, suggesting that there is a permissive component to CSF-1's effects on LK31C cells.

Even lineage-depleted D2 cells were heterogeneous in CD31 and Ly6C staining. Only by gating on individual subsets
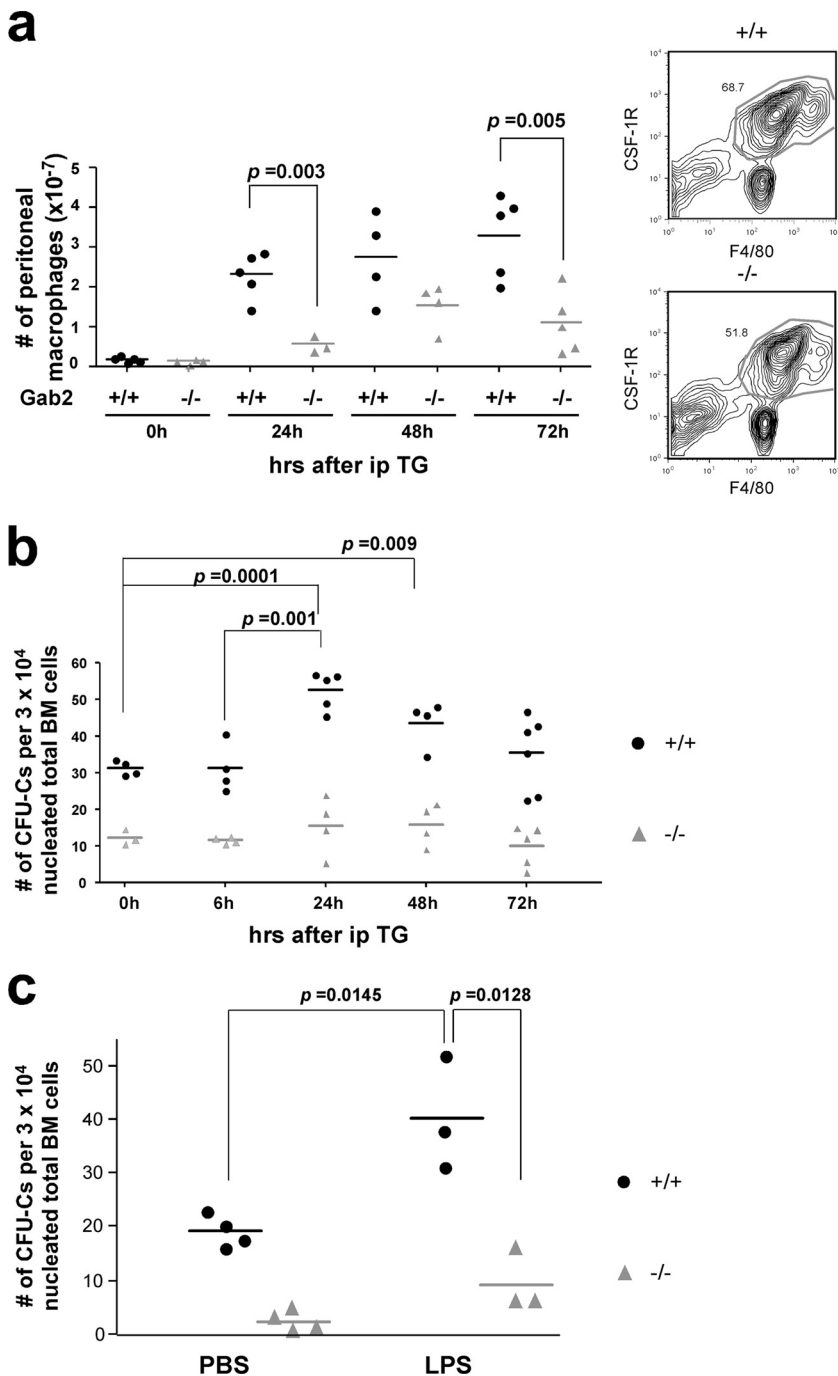
FIG. 12. Gab2$^{-/-}$ mice recruit fewer macrophages to the peritoneum after an inflammatory challenge, with an impaired BM CFU-C response. (a and b) Mice were injected with thioglycolate (TG). Peritoneal cells were counted and stained with CSF-1R and F4/80 antibodies to identify the macrophage population. At the time of sacrifice, total BM cells were also seeded for a CFU-C assay. (c) Mice were injected with LPS, and after 60 h, bone marrow was harvested for a CFU-C assay. (b and c) The differences in CFU-C between WT and −/− mice were significant at all time points. Data for individual mice are shown.

were deficiencies in CSF-1-mediated signaling revealed in Gab2$^{-/-}$ cells. LIN*$^-$ CD31^{high} Ly6C$^-$ progenitors from Gab2$^{-/-}$ mice showed diminished CSF-1-induced phosphorylation of Akt, S6, and Erk, consistent with Gab2's role in recruiting PI3K and SHP2 (19, 34). Simultaneous inhibition of the PI3K and Erk pathways was required to abolish S6 phos-

phorylation. By enhancing the activation of both the Akt and Erk pathways, Gab2 could be important for protein translation in CSF-1-responsive progenitors. E40K Akt seemed to be more effective in restoring CFU-C size than number, suggesting that upregulated Akt activity on its own could restore expansion to CFU that have committed to the MNP lineage.

HSCs deficient in PTEN have upregulated PI3K activity and show enhanced cycling leading to short-term expansion but long-term depletion (69). This might explain why E40K Akt is better able to restore colony expansion than increase the number of committed MNP progenitors. It has been suggested that the Akt and Erk pathways can influence myeloid cell commitment (5, 22). However, BM cells from Gab2$^{-/-}$ mice were not impaired in their ability to differentiate to Mϕs, supporting a role for Gab2 after commitment of HSCs to the myeloid lineage.

Unlike progenitors, BMMs did not require Gab2 for full activation of Akt or S6 although Gab2's role in PI3K-dependent, Akt-independent pathways is not excluded (28). In Gab2$^{-/-}$ BMMs, CSF-1-induced Erk and JNK1 phosphorylation was increased. This is opposite to findings in mast cells where c-Kit-dependent Rac/JNK activity was decreased (67). Thus, JNK1 is differentially regulated in the two cell types. Possibly, increased Gab1 and Gab3 levels contributed to the increase in Erk and JNK phosphorylation. The lack of an increase in MKK7 phosphorylation implies that Gab2 deficiency might impact JNK1 itself. The simultaneous upregulation in Erk and JNK1 phosphorylation suggests a linked mechanism, e.g., via DUSPs, many of which target both Erk and JNK. DUSP5, which is implicated in Mϕ differentiation, targets Erk but not JNK (17). In our experiments, a potential role for inducible DUSPs (e.g., DUSP1) to regulate the sustained phase is supported by the ability of AD to increase JNK1 phosphorylation in WT cells to that seen in Gab2$^{-/-}$ cells without any detectable effect on the Gab2$^{-/-}$ cells. As expected, AD did not influence the acute phase where noninducible DUSPs (e.g., DUSP16) would act. The pathway linking Gab2 to JNK1 in BMMs remains to be determined. Gab2 is a large protein, and to date, only a few interaction motifs have been confirmed (18a). Regardless, reduction of JNK1 levels modestly restored proliferation of Gab2$^{-/-}$ BMMs to that observed in WT cells, whereas almost complete ablation reduced CSF-1-dependent proliferation in both WT and Gab2$^{-/-}$ cells, thereby underscoring the importance of balanced JNK activity in BMMs. This conclusion is consistent with observations that JNK activity is linked to both proliferation and apoptosis (62). Although no short-term defect in CSF-1-mediated DNA synthesis was observed in JNK1$^{-/-}$ BMMs (49), the contrast with our findings could reflect compensatory changes in mice where JNK1 was deleted from conception versus acute knockdown in our cells.

In response to TG, Gab2$^{-/-}$ mice showed a significant reduction in recruited Mϕs. While a local proliferation or mobilization defect could not be excluded, the BM of WT mice responded to TG and LPS with an increase in CFU-C that was not observed in Gab2$^{-/-}$ mice. In this context, we point out that the body increases production of circulating CSF-1 dramatically in infection and inflammation (56), making CSF-1 a potential link between the BM and sites of inflammation.

Overall, our work highlights the importance of Gab2 in MNP development. In early MNP progenitors, in response to CSF-1, Gab2 acts through PI3K and Erk to promote proliferation and survival, while in terminal MNP development, Gab2 acts through JNK1 so that in the absence of Gab2, JNK1 is deregulated and inhibits proliferation. Through Gab2's modulation of MNP production, it could be a novel target for anti-inflammatory therapies.

REFERENCES

1. **Auffray, C., M. H. Sieweke, and F. Geissmann.** 2009. Blood monocytes: development, heterogeneity, and relationship with dendritic cells. Annu. Rev. Immunol. **27:**669–692.
1a. **Bartocci, A., J. W. Pollard, and E. R. Stanley.** 1986. Regulation of colony-stimulating factor 1 during pregnancy. J. Exp. Med. **164:**956–961.
2. **Böiers, C., et al.** 2010. Expression and role of FLT3 in regulation of the earliest stage of normal granulocyte-monocyte progenitor development. Blood **115:**5061–5068.
3. **Borsello, T., et al.** 2003. A peptide inhibitor of c-Jun N-terminal kinase protects against excitotoxicity and cerebral ischemia. Nat. Med. **9:**1180–1186.
4. **Bruhns, P., A. Samuelsson, J. W. Pollard, and J. V. Ravetch.** 2003. Colony-stimulating factor-1-dependent macrophages are responsible for IVIG protection in antibody-induced autoimmune disease. Immunity **18:**573–581.
5. **Buitenhuis, M., et al.** 2008. Protein kinase B (c-akt) regulates hematopoietic lineage choice decisions during myelopoiesis. Blood **111:**112–121.
6. **Centeno, C., et al.** 2007. Role of the JNK pathway in NMDA-mediated excitotoxicity of cortical neurons. Cell Death Differ. **14:**240–253.
7. **Chitu, V., and E. R. Stanley.** 2006. Colony-stimulating factor-1 in immunity and inflammation. Curr. Opin. Immunol. **18:**39–48.
8. **Cohen, P. E., K. Nishimura, L. Zhu, and J. W. Pollard.** 1999. Macrophages: important accessory cells for reproductive function. J. Leukoc. Biol. **66:**765–772.
9. **Dai, X. M., et al.** 2002. Targeted disruption of the mouse colony-stimulating factor 1 receptor gene results in osteopetrosis, mononuclear phagocyte deficiency, increased primitive progenitor cell frequencies, and reproductive defects. Blood **99:**111–120.
10. **Daly, R. J., et al.** 2002. The docking protein Gab2 is overexpressed and estrogen regulated in human breast cancer. Oncogene **21:**5175–5181.
11. **de Bruijn, M. F., et al.** 1994. Distinct mouse bone marrow macrophage precursors identified by differential expression of ER-MP12 and ER-MP20 antigens. Eur. J. Immunol. **24:**2279–2284.
12. **Duncan, A. W., et al.** 2005. Integration of Notch and Wnt signaling in hematopoietic stem cell maintenance. Nat. Immunol. **6:**314–322.
13. **Fleming, T. J., M. L. Fleming, and T. R. Malek.** 1993. Selective expression of Ly-6G on myeloid lineage cells in mouse bone marrow. RB6-8C5 mAb to granulocyte-differentiation antigen (Gr-1) detects members of the Ly-6 family. J. Immunol. **151:**2399–2408.
14. **Ginhoux, F., et al.** 2010. Fate mapping analysis reveals that adult microglia derive from primitive macrophages. Science **330:**841–845.
15. **Ginhoux, F., et al.** 2006. Langerhans cells arise from monocytes in vivo. Nat. Immunol. **7:**265–273.
16. **Gordon, S., and P. R. Taylor.** 2005. Monocyte and macrophage heterogeneity. Nat. Rev. Immunol. **5:**953–964.
17. **Grasset, M., S. Gobert-Gosse, G. Mouchiroud, and R. Bourette.** 2009. Macrophage differentiation of myeloid progenitor cells in response to M-CSF is regulated by the dual-specificity phosphatase DUSP5. J. Leukoc. Biol. **87:**127–135.
18. **Groblewska, M., et al.** 2007. Serum levels of granulocyte colony-stimulating factor (G-CSF) and macrophage colony-stimulating factor (M-CSF) in pancreatic cancer patients. Clin. Chem. Lab. Med. **45:**30–34.
18a. **Gu, H.** 2010. Gab2. UCSD-Nat. Mol. Pages http://www.signaling-gateway.org/molecule/query?afcsid=A002238.
19. **Gu, H., and B. G. Neel.** 2003. The 'Gab' in signal transduction. Trends Cell. Biol. **13:**122–130.
20. **Gu, H., J. Pratt, S. Burakoff, and B. Neel.** 1998. Cloning of p97/Gab2, the major SHP2-binding protein in hematopoietic cells, reveals a novel pathway for cytokine-induced gene activation. Mol. Cell **2:**729–740.
21. **Gu, H., et al.** 2001. Essential role for Gab2 in the allergic response. Nature **412:**186–190.

22. **Hsu, C. L., K. Kikuchi, and M. Kondo.** 2007. Activation of mitogen-activated protein kinase kinase (MEK)/extracellular signal regulated kinase (ERK) signaling pathway is involved in myeloid lineage commitment. Blood **110:**1420–1428.

23. **Hunter, M., et al.** 2009. Survival of monocytes and macrophages and their role in health and disease. Front. Biosci. **14:**4079–4102.

24. **Itoh, S., F. Yoshitake, H. Narita, K. Ishihara, and S. Ebisu.** 2007. Gab2 plays distinct roles in bone homeostasis at different time points. J. Bone Miner. Metab. **25:**81–85.

25. **Iwasaki, H., and K. Akashi.** 2007. Myeloid lineage commitment from the hematopoietic stem cell. Immunity **26:**726–740.

26. **Kalaitzidis, D., and B. Neel.** 2008. Flow-cytometric phosphoprotein analysis reveals agonist and temporal differences in responses of murine hematopoietic stem/progenitor cells. PLoS One **3:**e3776.

27. **Ke, Y., et al.** 2007. Role of Gab2 in mammary tumorigenesis and metastasis. Oncogene **26:**4951–4960.

28. **Lee, A. W., and D. J. States.** 2006. Colony-stimulating factor-1 requires PI3-kinase-mediated metabolism for proliferation and survival in myeloid cells. Cell Death Differ. **13:**1900–1914.

29. **Lee, A. W.-M.** 1999. Synergistic activation of mitogen-activated protein kinase by cyclic AMP and myeloid growth factors opposes cyclic AMP's growth-inhibitory effects. Blood **93:**537–553.

30. **Lee, A. W.-M., S. Nambirajan, and J. G. Moffat.** 1999. CSF-1-activates MAPK-dependent and p53-independent pathways to induce growth arrest of hormone-dependent human breast cancer cells. Oncogene **18:**7475–7492.

31. **Lee, A. W.-M., and D. J. States.** 2000. Both Src-dependent and -independent mechanisms mediate phosphatidylinositol 3-kinase regulation of colony stimulating factor 1-activated mitogen-activated protein kinases in myeloid progenitors. Mol. Cell. Biol. **20:**6779–6798.

32. **Leenen, P. J., M. F. de Bruijn, J. S. Voerman, P. A. Campbell, and W. van Ewijk.** 1994. Markers of mouse macrophage development detected by monoclonal antibodies. J. Immunol. Methods **174:**5–19.

33. **Liu, Y., B. Jenkins, J. L. Shin, and L. R. Rohrschneider.** 2001. Scaffolding protein Gab2 mediates differentiation signaling downstream of Fms receptor tyrosine kinase. Mol. Cell. Biol. **21:**3047–3056.

34. **Liu, Y., and L. R. Rohrschneider.** 2002. The gift of Gab. FEBS Lett. **515:**1–7.

35. **MacDonald, K. P., et al.** 2005. The colony-stimulating factor 1 receptor is expressed on dendritic cells during differentiation and regulates their expansion. J. Immunol. **175:**1399–1405.

36. **Mao, Y., and A. W. Lee.** 2005. A novel role for Gab2 in bFGF-mediated cell survival during retinoic acid-induced neuronal differentiation. J. Cell Biol. **170:**305–316.

37. **McNiece, I. K., B. E. Robinson, and P. J. Quesenberry.** 1988. Stimulation of murine colony-forming cells with high proliferative potential by the combination of GM-CSF and CSF-1. Blood **72:**191–195.

38. **Nishida, K., and T. Hirano.** 2003. The role of Gab family scaffolding adapter proteins in the signal transduction of cytokine and growth factor receptors. Cancer Sci. **94:**1029–1033.

39. **Patterson, K. I., T. Brummer, P. M. O'Brien, and R. J. Daly.** 2009. Dual-specificity phosphatases: critical regulators with diverse cellular targets. Biochem. J. **418:**475–489.

40. **Perez, O. D., and G. P. Nolan.** 2002. Simultaneous measurement of multiple active kinase states using polychromatic flow cytometry. Nat. Biotechnol. **20:**155–162.

41. **Perfetto, S. P., P. K. Chattopadhyay, and M. Roederer.** 2004. Seventeen-colour flow cytometry: unravelling the immune system. Nat. Rev. Immunol. **4:**648–655.

42. **Persons, D. A., et al.** 1997. Retroviral-mediated transfer of the green fluorescent protein gene into murine hematopoietic cells facilitates scoring and selection of transduced progenitors in vitro and identification of genetically modified cells in vivo. Blood **90:**1777–1786.

43. **Pixley, F. J., and E. R. Stanley.** 2004. CSF-1 regulation of the wandering macrophage: complexity in action. Trends Cell Biol. **14:**628–638.

44. **Pollard, J. W.** 2009. Trophic macrophages in development and disease. Nat. Rev. Immunol. **9:**259–270.

45. Reference deleted.

46. **Qian, B.-Z., and J. W. Pollard.** 2010. Macrophage diversity enhances tumor progression and metastasis. Cell **141:**39–51.

47. **Reiman, E. M., et al.** 2007. GAB2 alleles modify Alzheimer's risk in APOE epsilon4 carriers. Neuron **54:**713–720.

48. **Roth, P., and E. R. Stanley.** 1992. The biology of CSF-1 and its receptor. Curr. Top. Microbiol. Immunol. **181:**141–167.

49. **Sanchez-Tillo, E., et al.** 2007. JNK1 Is required for the induction of Mkp1 expression in macrophages during proliferation and lipopolysaccharide-dependent activation. J. Biol. Chem. **282:**12566–12573.

50. **Sasmono, R. T., et al.** 2003. A macrophage colony-stimulating factor receptor-green fluorescent protein transgene is expressed throughout the mononuclear phagocyte system of the mouse. Blood **101:**1155–1163.

51. **Seiffert, M., et al.** 2003. Gab3-deficient mice exhibit normal development and hematopoiesis and are immunocompetent. Mol. Cell. Biol. **23:**2415–2424.

52. **Stanley, E., L. Guilbert, R. Tushinski, and S. Bartelmez.** 1983. CSF-1—a mononuclear phagocyte lineage-specific hemopoietic growth factor. J. Cell. Biochem. **21:**151–159.

53. **Stanley, E. R.** 2009. Lineage commitment: cytokines instruct, at last! Cell Stem Cell **5:**234–236.

54. **Stanley, E. R.** 1997. Murine bone marrow-derived macrophages. Methods Mol. Biol. **75:**301–304.

55. **Sugatani, T., and K. A. Hruska.** 2005. Akt1/Akt2 and mammalian target of rapamycin/Bim play critical roles in osteoclast differentiation and survival, respectively, whereas Akt is dispensable for cell survival in isolated osteoclast precursors. J. Biol. Chem. **280:**3583–3589.

56. **Sweet, M. J., and D. A. Hume.** 2003. CSF-1 as a regulator of macrophage activation and immune responses. Arch. Immunol. Ther. Exp. (Warsz). **51:**169–177.

57. **Tagoh, H., et al.** 2002. Transcription factor complex formation and chromatin fine structure alterations at the murine c-fms (CSF-1 receptor) locus during maturation of myeloid precursor cells. Genes Dev. **16:**1721–1737.

58. **Taylor, P. R., et al.** 2005. Macrophage receptors and immune recognition. Annu. Rev. Immunol. **23:**901–944.

59. **Van Furth, R., M. C. Diesselhoff-den Dulk, and H. Mattie.** 1973. Quantitative study on the production and kinetics of mononuclear phagocytes during an acute inflammatory reaction. J. Exp. Med. **138:**1314–1330.

60. **Vivanco, I., et al.** 2007. Identification of the JNK signaling pathway as a functional target of the tumor suppressor PTEN. Cancer Cell **11:**555–569.

61. **Wada, T., et al.** 2005. The molecular scaffold Gab2 is a crucial component of RANK signaling and osteoclastogenesis. Nat. Med. **11:**394–399.

62. **Wada, T., and J. M. Penninger.** 2004. Mitogen-activated protein kinases in apoptosis regulation. Oncogene **23:**2838–2849.

63. **Wei, S., et al.** 2010. Functional overlap but differential expression of CSF-1 and IL-34 in their CSF-1 receptor-mediated regulation of myeloid cells. J. Leukoc. Biol. **88:**495–505.

64. **Wiktor-Jedrzejczak, W., and S. Gordon.** 1996. Cytokine regulation of the macrophage (M phi) system studied using the colony stimulating factor-1-deficient op/op mouse. Physiol. Rev. **76:**927–947.

65. **Wiktor-Jedrzejczak, W., et al.** 1992. CSF-1 deficiency in the op/op mouse has differential effects on macrophage populations and differentiation stages. Exp. Hematol. **20:**1004–1010.

66. **Xu, D., et al.** 2010. A gain-of-function mutation in Ptpn11 (Shp-2) phosphatase induces myeloproliferative disease by aberrant activation of hematopoietic stem cells. Blood **116:**3611–3621.

67. **Yu, M., C. A. Lowell, B. G. Neel, and H. Gu.** 2006. Scaffolding adapter Grb2-associated binder 2 requires Syk to transmit signals from Fc{epsilon}RI. J. Immunol. **176:**2421–2429.

68. **Yu, M., et al.** 2006. The scaffolding adapter Gab2, via Shp-2, regulates Kit-evoked mast cell proliferation by activating the Rac/JNK pathway. J. Biol. Chem. **281:**28615–28626.

69. **Zhang, J., et al.** 2006. PTEN maintains haematopoietic stem cells and acts in lineage choice and leukaemia prevention. Nature **441:**518–522.

70. **Zhang, Y., et al.** 2007. Abnormal hematopoiesis in Gab2 mutant mice. Blood **110:**116–124.